University of Alberta

The Effect of Stretch on Gas Sorption in Rubber

by

Lei Ji

A thesis submitted to the Faculty of Graduate Studies and Research in partial fulfillment of the requirements for the degree of *Master of Science*

Department of *Mechanical Engineering*

Edmonton, Alberta
Spring 2006

Your file Votre référence
ISBN: 0-494-13833-5
Our file Notre référence
ISBN: 0-494-13833-5

University of Alberta

Library Release Form

Name of Author: *Lei Ji*

Title of Thesis: *The Effect of Stretch on Gas Sorption in Rubber*

Degree: *Master of Science*

Year this Degree Granted: *2006*

_____

Signature

Abstract

A better understanding of gas sorption in rubbers is desired since the rubbers are often used in high pressure environments under stress. A polymer solution is formed when gas is absorbed by a polymer and will result in changes in physical dimensions and possibly, mechanical properties. When pressure is released, permanent deformation or damage may occur in the polymer.

In this study, a desorption method was developed to measure CO_2 sorption in silicone rubber and EPDM under uni-axial stretch. A thermodynamic model was developed to predict the gas sorption in rubber under uni-directional stretch, and combines the work of Flory-Huggins theory for mixing and Ogden's model for rubber elasticity deformation.

Test results show that higher stretch ratios will lead to higher gas solubility in rubber. Furthermore, the effect is greater for rubber with higher shear modulus. Also, the stretch has no significant effect on gas partial molar volume and the Flory-Huggins parameter.

Acknowledgements

I am particularly indebted to my supervisors, Dr. T. W. Forest and Dr. P.-Y. Ben Jar for their guidance and financial support throughout this study.

I would like to thank Mr. Bernie Faulkner and Mr. Ian Buttar who offered me excellent technical help and precious discussions.

My appreciation goes to the members of the Durable Materials Research Lab: Mr. Chengye Fan, Mr. Yemi Setiadi, Mr. Hyock-Ju Kwon, Dr. T. Kuboki, Mr. Tadayoshi Yamanaka, and Miss. Tik for their friendship and provision of a pleasant environment.

Finally, my gratitude must be given to my wife, Ms Hongyan Yang, my son, Austin Ji, and my parents, Guangao Ji and Aiping Yang for their encourage and support throughout the study.

Table of Contents

List of Tables

List of Figures

List of Symbols

A	Surface area of the rubber sample
B , ΔB	Gibbs free energy and the change of Gibbs free energy
C , C_1, C_0	Gas concentration, surface concentration, and initial concentration
C_{ijpq}	Elastic coefficient
D	Diffusion coefficient
E	Young's Modulus
f	Force
F , ΔF , ΔF_m , ΔF_d	Helmholtz free energy, the total free energy change, free energy change due to mixing and deformation
G	Shear Modulus
k	Boltzmann's constant
K	Henry's law constant
L	Length
n_1 , n_2	The number of moles of a solute and solvent
N_1 , N_2	Number of molecules of solute and solvent
P , P_0	Pressure and vapor pressure of gas
p_{12}	The number of solvent-polymer segment contacts in the solution
S , ΔS , ΔS_m	Entropy, entropy change, and entropy change due to Mixing
T	Temperature
U , ΔU , ΔU_m	Internal energy, the change of internal energy, and change

	of internal energy due to mixing
V, V_0	Volume and undeformed volume
V_g	Partial molar volume
w_{CO_2}	CO_2 mass fraction in polymer solution
W	Strain-energy function
x	The number of segments of each polymer chain, the size of each segment is equal to a solute molecules
$\phi_1,\ \phi_2$	Solute and solvent volume fraction
χ	Flory-Huggins parameter
$\sigma,\ \sigma_n$	The principle Cauchy stress and nominal stress
ε_{ij}	Strain
γ	Gas activity coefficient
$\mu_1, \mu_2,\ \mu_1^0$	Chemical potential of solute and solvent, and solute chemical potential at initial state
$\lambda, \lambda_x,\ \lambda_y, \lambda_z$	Stretch ratio, stretch ratios in X, Y and Z-directions
$\Omega_1, \Omega_2,\ \Omega_{12}$	The number of spatial arrangements of molecules in the the pure solute, pure solvent and ideal mixture
$\alpha_1,\ \alpha_2$	Coefficients of the Ogden's equation
$\eta_1,\ \eta_2$	Coefficients of the Ogden's equation
Λ	Volume dilation ratio
β	Linear dilation ratio
δ_{ij}	Hydrostatic pressure tensor

1. Introduction

1.1 Introduction

Polymers have been used in a wide variety of applications from automobile parts to structural elements. In many of these applications, the polymer is exposed to solvents at elevated pressures. Over a long period of exposure, these solutes will dissolve into the polymer, forming a polymer solution that will result in changes in physical dimensions and possibly mechanical properties. When the pressure is released, permanent deformation or damage may occur. A polyurethane rubber sample that had been previously placed in a high pressure was severely damaged after being depressurized as shown in Fig. 1-1 [1].

Fig. 1-1 Surface cracks on an explosively decompressed polyurethane rubber specimen [1]

Sometimes, the polymers are used at higher pressures with arbitrary stresses, such as polymer linings with some residue stresses used for oil pipelines to prevent corrosion.

When the pipeline is depressurized, the linings will be deformed and detached from the pipe wall due to the build-up pressure in the annulus, the swelling of linings caused by thermal effects and gas condensate absorption. Figure 1-2 shows a deformed medium density polyethylene lining used in an oil pipeline [2].

(a) Longitudinal section (b) Cross section

Fig. 1-2 Schematic of the deformed polymer lining after being depressurized [2]

When solutions are mentioned, we often think of liquid solutions, while solutions may exist in liquid, gas and solid phases. By definition, a solution is a homogeneous mixture of two or more substances. A rubbery polymer/gas solution is the main topic in this study, where the solvent is the polymer and the solute is the gas component.

1.2 Literature Review

Over the past several decades, many analytical and experimental investigations on gas sorption in polymers have been carried out. However, among those works, the polymers were mostly in a stress-free state.

Fleming and Koros [3] measured the carbon dioxide sorption isotherm in silicone rubber at 35°C. Their research showed that at low gas concentrations or low

pressures, the sorption isotherm can be explained by a Henry's law prediction as shown in Fig. 1-3:

$$C = KP \tag{1-1}$$

where C is the concentration of the sorbed gas in units of cm^3 (STP)/ (cm^3 polymer), K is the Henry's law constant in units of cm^3 (STP)/ (cm^3 polymer MPa), and P is the gas pressure in MPa.

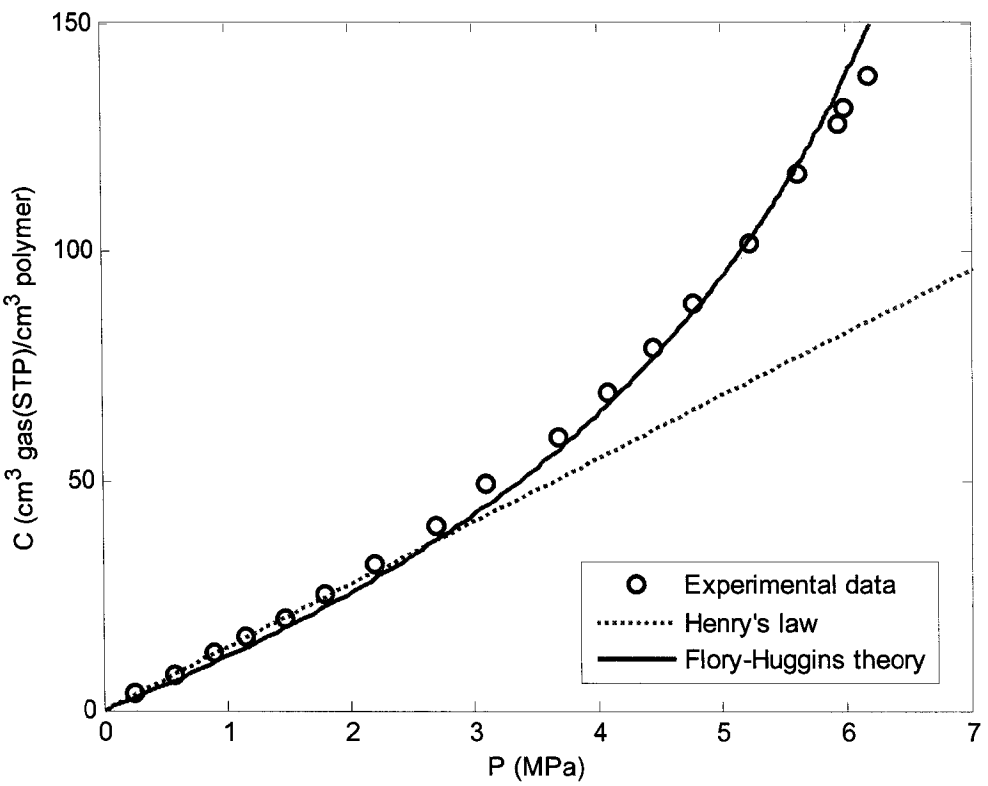

Fig. 1-3 Silicone rubber/CO_2 sorption isotherm at 35°C measured by Fleming and Koros. Above a measurement of 3 MPa, apparent deviations from Henry's law were observed, and the deviation was predicted by a Flory-Huggins equation as shown in Eqn. 1-2.

$$\ln\left(\frac{P}{P_0}\right) = \ln(1-\phi_2) + \phi_2 + \chi\phi_2^{\,2} \tag{1-2}$$

where P is the penetrant pressure, P_0 is the gas vapor pressure at the experimental temperature, ϕ_2 are the volume fraction of polymer, and χ is the Flory-Huggins parameter. The Flory-Huggins prediction was also plotted in Fig. 1-3 for comparison with Henry's law prediction and experimental data. The figure shows that the Flory-Huggins prediction was in good agreement with measured gas concentration for pressures up to $5.6\,MPa$. Isotropic dilation of silicone rubber upon gas absorption was also observed by measuring the linear dilation in the vertical and horizontal dimensions. In addition, the partial molar volume of the carbon dioxide was found to be constant with a value of $46\,cm^3/mol$ for carbon dioxide concentration up to 78 cm^3 gas (STP)/ (cm^3 polymer).

Many other researchers [7-16] conducted investigations on various gas sorption isotherms in different rubbery and glassy polymers. For rubbery polymers, most of the research was based on the Flory-Huggins theory and the polymers were in stress-free state, while the studies on glassy polymers are beyond the scope of this study. The purpose of this literature review is intended to point out the major trend of the research work on gas sorption in rubbery polymers, but not to cover all works published in the past.

Lipscomb [4] developed a macroscopic thermodynamic model of gas sorption in polymer with an arbitrary small stress where the deformation is elastic. The polymer sample is taken from some reference pressure and arbitrary small stress state to the pressure of the sorption experiment; then the sample is deformed to accommodate the dilation associated with the gas solute at constant temperature and pressure; finally, sorption equilibrium is reached. Lipscomb assumed small, homogeneous elastic deformation, reversible processes and isothermal conditions.

The free energy was calculated as the sum of a term due to deformation of the solid polymer structure (to permit the inclusion of the gas solute) and a term due to mixing of the gas in the deformed polymer matrix. The approach in this study is similar to this work and the details are given in Chapter 2. The thermodynamics of the deformation assumed that the polymer is an elastic solid, instead of a cross-linked rubber. Mixing was described by the same relationship used in the Flory-Huggins theory.

The Gibbs free energy change associated with deformation was expressed as:

$$\Delta B_{Deform} = V_0 \int_{\varepsilon} [(\sigma_{ij})_0 + (C_{ijpq})_0 \varepsilon_{pq} + P\delta i_j] d\varepsilon_{ij} + \int_{p} V dP + 0(\varepsilon_{ij}{}^3) \qquad (1\text{-}3)$$

where V_0 is the original volume of the polymer, σ_{ij} is the stress, $\varepsilon_{ij}\,(i, j = 1, 2, 3)$ are the strains, C_{ijpq} is the isothermal elastic coefficient, P is the pressure, and the subscript 0 refers quantities to the undeformed state. The term $P\delta_{ij}$ is the hydrostatic pressure in the polymer and δ_{ij} is defined as

$$\delta_{ij} = \begin{vmatrix} 1 & 0 & 0 \\ 0 & 1 & 0 \\ 0 & 0 & 1 \end{vmatrix}$$

The Gibbs free energy change associated with mixing the deformed polymer and gas was calculated through a Flory-Huggins treatment:

$$\Delta B_{Mix} = kT[N_1 \ln(\phi_1) + N_2 \ln(\phi_2) + \chi N_1 \phi_2] \qquad (1\text{-}4)$$

where N_1 and N_2 are the numbers of sorbed gas and polymer molecules, respectively; ϕ_1 and ϕ_2 are the volume fractions of gas solute and polymer, respectively; χ is the Flory-Huggins parameter, k is the Boltzmann's constant and T is the temperature in Kelvin.

The total change of Gibbs free energy, ΔB, was given by the sum of the Gibbs

free energy changes due to deformation and mixing. At equilibrium, equating the chemical potential of the gas in the pure gas state and that in the polymer, the sorption isotherm becomes

$$\mu_1 - \mu_1^{\,0} = \left(\frac{\partial(\Delta B)}{\partial N_1}\right)_{T,P,N_2} = kT\ln\left(\frac{\gamma P}{P_{Rs}}\right) \tag{1-5}$$

where μ_1 and $\mu_1^{\,0}$ are the chemical potentials of the absorbed gas at pressure P and reference pressure P_{Rs} respectively, and γ is the activity coefficient.

Flory [5, 6] constructed a model of swelling of a polymer network when saturated with a liquid solute. He investigated the equilibrium swelling of a cubic polymer gel that was under a tensile force f in the direction as shown in Fig. 1-4, when in contact with material that dissolves in the polymer. The initial state, with Helmholtz free energy, F_0, is: (1) an un-deformed polymer network (free of solute) made up of N_2 chains, each with x segments of solute molecule size, with volume $V_0 = L_0^{\,3} = xN_2v_m$, where v_m is the volume occupied by a solute molecule and L_0 is the un-swollen edge; and (2) N_1 molecules of solute with volume N_1v_m. The final state is the network swollen with N_1 molecules of solute, with volume (assumed additive) given as

$$V = (N_1 + xN_2)v_m$$

and the dimensions are expressed as:

$$L_x = L = \lambda L_0,\ L_y = L_z = \left(\frac{V}{L}\right)^{1/2} \tag{1-6}$$

where λ is the linear stretch ratio in X-direction (due to tensile force and swelling). The volume swelling ratio is defined as:

$$\frac{V}{V_0} = \frac{1}{\phi_2} \tag{1-7}$$

where ϕ_2 is polymer volume fraction. Substituting Eqn. 1-7 in Eqn. 1-6 yields

$$\lambda_y = \lambda_z = \frac{1}{(\lambda\phi_2)^{1/2}},$$

where λ_y and λ_z are the linear stretch ratios in the Y and Z-directions respectively (due to tensile force and swelling).

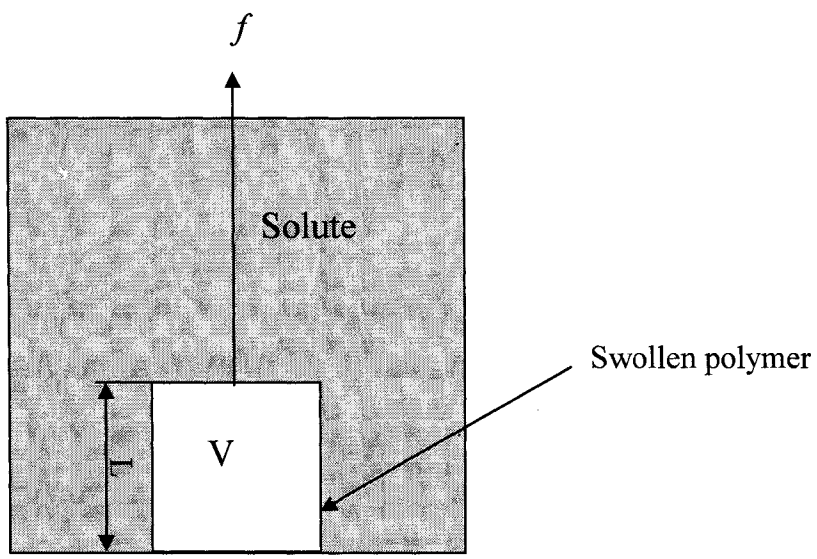

Fig. 1-4 Flory's swelling model of polymer gel under a tensile force (Hill, [5])

The model assumes that the Helmholtz free energy changes due to mixing and deformation are independent of each other. The total Helmholtz free energy change is given as

$$\Delta F = \Delta F_m + \Delta F_d \tag{1-8}$$

where ΔF_m and ΔF_d are the Helmholtz free change due to mixing and deformation,

respectively. The ΔF_m is obtained from the Flory-Huggins theory,

$$\Delta F_m = kT\left[N_1 \ln \phi_1 + N_2 \ln \phi_2 + \chi N_1 \phi_2\right]$$

Assuming that the rubber is perfectly elastic and neglecting the PdV work at atmospheric pressure. The deformation portion, ΔF_d, is obtained from the definition of the Helmholtz free energy,

$$\begin{aligned} dF_d &= dU_d - d(TS_d) \\ &= fdL + TdS_d + \mu_2 dN_2 - TdS_d - S_d dT \\ &= fdL - S_d dT + \mu_2 dN_2 \end{aligned} \tag{1-9}$$

where f is the tensile force. The second term in Eqn. 1-9, $S_d dT$ disappears because the temperature is kept constant, while $\mu_2 dN_2$ is zero too since N_2 is constant. Taking the partial derivatives with respect to T and L yields

$$\frac{\partial}{\partial T}\left(\frac{\partial F_d}{\partial L}\right)_T = \frac{\partial}{\partial L}\left(\frac{\partial F_d}{\partial T}\right)_\lambda$$

This leads to

$$\left(\frac{\partial S_d}{\partial L}\right)_T = -\left(\frac{\partial f}{\partial T}\right)_\lambda \tag{1-10}$$

Neglecting the PdV work at atmospheric pressure, the differential internal energy dU is given by

$$dU = TdS + fdL + \mu_2 dN_2 \tag{1-11}$$

The last term of the Eqn. 1-11 disappears since N_2 is constant. Taking partial derivatives with respect to L at constant temperature yields

$$\left(\frac{\partial U}{\partial L}\right)_T = f + T\left(\frac{\partial S}{\partial L}\right)_T = f - T\left(\frac{\partial f}{\partial T}\right)_\lambda \tag{1-12}$$

Anthony, Caston, and Guth [32] showed by measurement that $\left(\frac{\partial U}{\partial L}\right)_T$ is approximately zero; thus, the elasticity of rubber is purely an entropy effect. Substituting Eqn. 1-10 and $\left(\frac{\partial U}{\partial L}\right)_T = 0$ into Eqn. 1-12 yields

$$f = -T\left(\frac{\partial S_d}{\partial L}\right)_T \tag{1-13}$$

Keeping temperature constant, Eqn. 1-13 becomes

$$fdL = -TdS_d \tag{1-14}$$

Substituting Eqn. 1-14 and $S_d dT = 0$ into Eqn. 1-9, the Helmholtz free energy change due to deformation is obtained as

$$\Delta F_d = -T\Delta S_d \tag{1-15}$$

Wall's theory [5, 33] of rubber elasticity, which is based on a Gaussian distribution of the polymer chains, was employed to calculate ΔS_d:

$$\Delta S_d = \frac{N_2 k}{2}\left[\ln(\lambda_x\lambda_y\lambda_z) - \lambda_x^{\,2} - \lambda_y^{\,2} - \lambda_z^{\,2} + 3\right] \tag{1-16}$$

For uni-directional stretch, define $\lambda_x = \lambda$ that leads to $\lambda_y = \lambda_z = \frac{1}{(\lambda\phi_2)^{1/2}}$. Substituting λ_x, λ_y and λ_z into Eqn. 1-16 yields

$$\Delta S_d = \frac{N_2 k}{2}\left[\ln\left(\lambda \times \frac{1}{\lambda\phi_2}\right) - \lambda^2 - \frac{2}{\lambda\phi_2} + 3\right]$$

$$= \frac{N_2 k}{2}\left(-\ln\phi_2 - \lambda^2 - \frac{2}{\lambda\phi_2} + 3\right) \tag{1-17}$$

where N_2 is the number of chains of rubber, k is the Boltzmann's constant, and λ is

stretch ratio.

Substituting Eqn. 1-17 into Eqn. 1-15 yields an expression for ΔF_d in terms of λ. Finally, substituting ΔF_d and ΔF_m into Eqn. 1-8, the total Helmholtz free energy change is

$$\frac{\Delta F}{kT} = N_1 \ln\phi_1 + N_2 \ln\phi_2 + \chi N_1 \phi_2 + \frac{N_2}{2}\left(\ln\phi_2 + \lambda^2 + \frac{2}{\lambda\phi_2} - 3\right)$$

At equilibrium, equating the solute chemical potential in the pure phase and in the polymer phase yields

$$\frac{\mu_1(\phi_2) - \mu_1(0)}{kT} = \left(\frac{\partial \Delta F / kT}{\partial N_1}\right)_{T,\lambda,N_2}$$

$$= \ln(1-\phi_2) + \phi_2 + \chi\phi_2^{\,2} + \frac{1}{x}\left(\frac{1}{\lambda} - \frac{\phi_2}{2}\right) = 0 \qquad (1\text{-}17)$$

where $\mu_1(\phi_2)$ and $\mu_1(0)$ are the chemical potentials of the solute in polymer and in pure phase respectively. In Flory's model of gel swelling, the overall deformation due to both the external force and swelling were considered to calculate the Helmholtz free energy change.

1.3 Scope of This Study

The structure of Flory's model was adopted in this study, and the Helmholtz free energy was chosen to be the appropriate thermodynamic potential because the total volume of gas and rubber and the temperature are kept constant. The objective of this study is to develop a thermodynamic model of gas sorption in rubber under stretch; design a test method to measure gas sorption; measure rubber dilation upon gas sorption; compare experimental data with the model predictions.

Chapter 2 describes the thermodynamic model developed for gas sorption in

stretched rubbers. The Flory-Huggins theory and Ogden's model of rubber elasticity will be used to develop the model.

Chapter 3 describes the methodology that was developed to measure gas sorption isotherms in rubbery polymers under uni-axial tension. The rubbery polymers used in the tests are silicone rubber and ethylene propylene diene monomer (EPDM), and the solute is CO_2 gas. The data process is also presented in this section.

Chapter 4 presents the test results and comparison with theoretical predictions. First, the coefficients of the Ogden's equation of rubber stress-strain relationship are determined to fit the force-elongation curve. Second, the test method is verified by comparing the test result with literature value for the zero stretch case. Finally, the experimental data are compared with theory.

The conclusions and recommendations of the future work are presented in the Chapter 5.

2. Theory of Gas Sorption in Rubber with Deformation

2.1 Introduction

As mentioned in previous chapter, Flory set up a model to explain the swelling of polymer gel when it is in contact with a solute and under a uni-directional tensile force. In Flory's model, the total Helmholtz free energy change was divided into two parts; one is the free energy change upon mixing obtained by a Flory-Huggins treatment, while the other part is the free energy change due to deformation, based on the Wall's theory of rubber elasticity.

The structure of Flory's model was adopted. The Flory-Huggins theory, since it has been verified by many researchers [3, 7-17], was kept in this study. Wall's theory of rubber elasticity, based on the assumption that rubber chains are randomly distributed, is valid only for "ideal rubber". There is only one parameter, the number of chains per unit volume that can be used to fit the theory to the force-stretch curve. For the rubbery polymers used in this study, the Wall's theory gave a poor fit to the data. Thus, Ogden's treatment, an empirical model, was adopted to calculate the Helmholtz free energy change due to deformation.

2.2 Flory-Huggins Theory

Gas sorption in rubbery polymer is characterized by sorption isotherms that are nearly linear in the low concentration range, followed by an upward curvature in the concentration-pressure curve at higher concentration range. Such a behavior is described by the Flory-Huggins theory:

$$\ln\left(\frac{P}{P_0}\right) = \ln(1-\phi_2) + \phi_2 + \chi\phi_2^{\,2} \qquad (2\text{-}1)$$

where P is the gas pressure, P_0 is the gas vapor pressure at the temperature of the experiment, ϕ_1 and ϕ_2 are the volume fractions of solute and polymer, respectively; χ is the Flory-Huggins parameter.

The Flory-Huggins theory developed independently by Flory and Huggins in 1942 is a direct generalization of the Bragg-Williams approximation of the lattice model of binary solutions [5]. The Bragg-Williams model is appropriate for solutions of molecules of equal size; each site in the lattice can be occupied by either an A molecule, represented by a circle, or a B molecule, denoted as a solid circle as shown in two dimensions in Fig. 2-1 (a). Since the polymer molecules are much larger than the solute molecules (a factor of usually 10^3 or 10^4), the Bragg-Williams approximation needs to be modified in order to apply it to polymer/solute solutions.

Flory and Huggins treated the polymer molecules as chains of segments, with each chain containing x segments, and each segment being equal in size to a solute molecule. On this basis it is possible to place solute molecules and segments of polymer chains in a lattice consisting of identical cells. Each lattice cell is occupied by either a solute molecule or a chain segment, and each polymer molecule is placed in the lattice so that its chain segments occupy a continuous sequence of x cells as shown in Fig. 2-1 (b).

By definition, the Helmholtz free energy, F is given by

$$F = U - TS$$

and the differential Helmholtz free energy is

$$dF = dU - TdS - SdT \tag{2-2}$$

where U is the internal energy, T is the temperature and S is the entropy. Under isothermal conditions, the last term on the right hand side of Eqn. 2-2 disappears and the

equation becomes

$$dF = dU - TdS \tag{2-3}$$

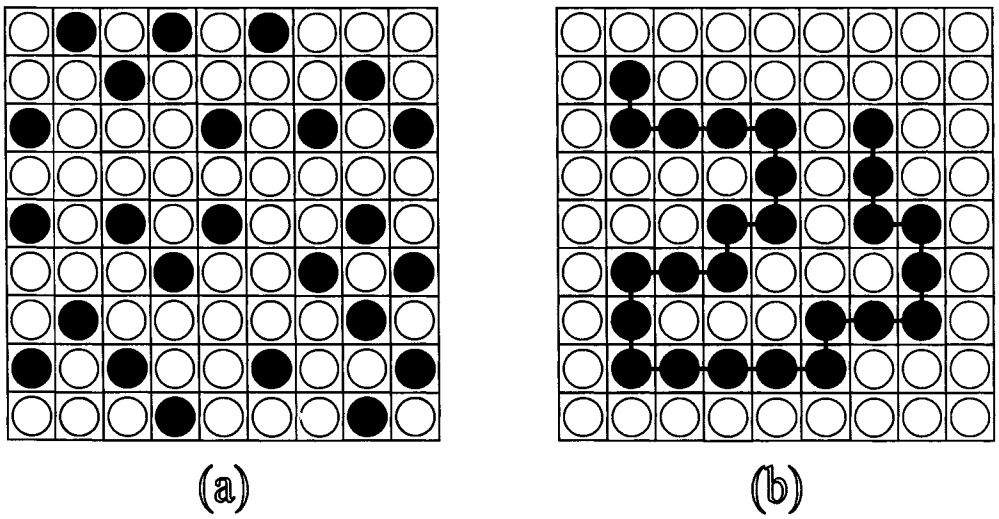

Fig. 2-1 Schematic representation of lattice, (a) mixture of molecules of equal size, (b) mixture of solute molecules with polymer molecules.

In order to obtain the change of Helmholtz free energy, the change of internal energy and entropy must be determined. The entropy change of mixing can be derived using statistical mechanical theories. The fundamental relation between the entropy S and the total number spatial configurations of the molecules, Ω is given by Boltzmann's equation [33].

$$S = k\ln(\Omega)$$

$$\Delta S_m = k[\ln(\Omega_{12}) - \ln(\Omega_1) - \ln(\Omega_2)]$$

where k is Boltzmann's constant, Ω_1, Ω_2 and Ω_{12} are the total numbers of the spatial arrangements of the molecules in the pure solvent, the pure solute and the ideal mixture

respectively, and the subscript m represents mixing. Since all molecules of the pure substance are identical, there is only one distinguishable spatial configuration; thus, $\ln(\Omega_1) = 0$ and , ΔS_m becomes

$$\Delta S_m = k \ln\left(\Omega_{12} / \Omega_2\right) \tag{2-4}$$

Since the Flory-Huggins theory is well known, the detailed information can be found in Flory's book [6], and will not be presented here.

Assuming a mean-field approximation of rubber chains, the entropy change of mixing can be expressed as:

$$\Delta S_m = -k\left[N_1 \ln \phi_1 + N_2 \ln \phi_2\right] \tag{2-5}$$

where N_1 and N_2 are the numbers of molecules of the solvent and solute, and ϕ_1 and ϕ_2 are the volume fractions of solute and solvent, respectively.

$$\phi_1 = \frac{N_1}{N_1 + xN_2}, \quad \phi_2 = \frac{xN_2}{N_1 + xN_2}$$

The internal energy change due to the random mixing, which is the basis of Bragg-Williams theory, must be calculated. Since the interaction drops quickly when the distance between the molecules increases, only the interaction between nearest molecules or chain segments is considered. Let u_{11} be the interaction energy between nearest neighbor solvent molecules, u_{22} between nearest polymer chain segments (not chemically bonded), and u_{12} between one solute molecule and one polymer chain segment. For every two solute-chain segment contacts formed on mixing, one solvent-solvent and one segment-segment contact of the pure component are lost. Thus, the internal energy change for the formation of a single solvent-segment contact, Δu_{12}, is given by

$$\Delta u_{12} = u_{12} - \frac{1}{2}(u_{11} + u_{22})$$

Define the internal energy change as

$$\Delta U_m = p_{12}\Delta u_{12}$$

where p_{12} is the total number of solute–segment contacts in the solution. Neglecting the chain end effects, and assuming each lattice site has z nearest sites, the total number of lattice sites adjacent to the polymer molecules is $(z-2)xN_2$, of which $(z-2)xN_2\phi_1$ are occupied by solvent molecules. Thus, p_{12} is obtained as

$$p_{12} = (z-2)xN_2\phi_1$$

$$= (z-2)N_1\phi_2$$

Thus, ΔU_m becomes

$$\Delta U_m = (z-2)N_1\phi_2\Delta u_{12}$$

The Flory-Huggins parameter, χ, is defined as, $\chi = \frac{(z-2)}{kT}\Delta u_{12}$. It is important to note that χ depends on temperature and polymer volume fraction. Thus, the internal energy of mixing becomes

$$\Delta U_m = kTN_1\phi_2\chi \qquad (2\text{-}6)$$

Substituting Eqns. 2-5 and 2-6 into Eqn 2-3, the Helmholtz free energy change due to mixing is obtained as:

$$\Delta F_m = kTN_1\phi_2\chi + kT(N_1 \ln\phi_1 + N_2 \ln\phi_2) \qquad (2\text{-}7)$$

The change of gas chemical potential is obtained by taking partial derivative of Eqn. 2-7 with respect to N_1,

$$\left(\frac{\partial(\Delta F_m)}{\partial N_1}\right)_{T,V,N_2} = kT\left[\ln(1-\phi_2)+\phi_2+\chi\phi_2^{\,2}\right]$$

At equilibrium, equating the chemical potential of the solute in the pure gas phase to that in the polymer solution yields the following equation,

$$kT\ln\frac{P}{P_0} = \mu_1^{\,P} - \mu_1^{\,0} = \ln(1-\phi_2)+\phi_2+\chi\phi_2^{\,2}$$

where $\mu_1^{\,P}$ and $\mu_1^{\,0}$ are the chemical potential of the solute in its solution at pressure P and pure solute state at vapor pressure at 20°C.

Although the Flory-Huggins theory gives quite a good prediction for gas sorption in rubbery material, it assumes no volume change upon mixing, which is unrealistic. Also the mathematical procedure used to calculate the total number of possible conformations of a polymer molecule in the lattice does not exclude self-intersections, which is clearly physically unrealistic. Furthermore, the theory is satisfactory only when polymer volume fraction is high.

2.3 Ogden's Model for Rubber Elasticity

Traditional strain energy functions of rubbery elasticity, such as Wall's theory [5, 33], Mooney's theory [27], and Rivlin's formulation [28] do not give a very good prediction of the force-stretch relationship at large deformations. Ogden [24] proposed an empirical approximation that yields good agreement with experimental data; thus, it was employed to describe the force-stretch relationship for the rubbery polymers used in this study.

Ogden assumed ideal rubber which is incompressible, homogeneous and isotropic in the undistorted state, perfectly elastic, and without any hysteresis effect. Based on these assumptions, the strain-energy function, W is given as

$$W = \sum_{r=1}^{n} \eta_r (\lambda_1^{\alpha_r} + \lambda_2^{\alpha_r} + \lambda_3^{\alpha_r} - 3)/\alpha_r \tag{2-8}$$

where λ_1, λ_2, and λ_3 are stretch ratios in X, Y and Z-directions, and η_r and α_r are constants to be determined.

The principle Cauchy stress (true stress based on actual area), σ_i is given by

$$\sigma_i = \lambda_i \frac{\partial W}{\partial \lambda_i} - P \qquad (i = 1,\ 2,\ 3) \tag{2-9}$$

where P is an arbitrary hydrostatic pressure introduced because of the incompressibility constraint. Substituting Eqn. 2-8 in Eqn.2-9, the principle Cauchy stresses are

$$\sigma_i = \sum_{r=1}^{n} \eta_r \lambda_i^{\alpha_r} - P \quad (i = 1,\ 2,\ 3) \tag{2-10}$$

In terms of uni-axial extension, defining $\lambda_1 = \lambda$ and $\sigma_1 = \sigma$, σ_2 and σ_3 are zero, the incompressible property leads to

$$\lambda_1 \lambda_2 \lambda_3 = 1 \text{ and } \lambda_2 = \lambda_3 = \lambda^{-\frac{1}{2}} \tag{2-11}$$

Substituting σ_1, σ_2, σ_3 and λ_1, λ_2, λ_3 into Eqn. 2-10 yields

$$\sigma = \sum_{r=1}^{n} \left(\eta_r \lambda^{\alpha_r}\right) - P \quad \text{and} \quad 0 = \sum_{r=1}^{n} \left(\eta_r \lambda^{-\frac{1}{2}\alpha_r}\right) - P$$

Elimination of P yields

$$\sigma = \sum_{r=1}^{n} \eta_r \left(\lambda^{\alpha_r} - \lambda^{-\frac{1}{2}\alpha_r}\right)$$

The nominal stress, σ_n based on the area of original cross section, is obtained by

$$\sigma_n = \frac{f}{A_0}$$

while the principle Cauchy stress is based on the area of the deformed cross section

$$\sigma = \frac{f}{A} = \frac{f}{L_{1y}L_{1z}} = \frac{f}{L_{0y}L_{0z}(\lambda^{-\frac{1}{2}})^2} = \frac{f}{A_0}\lambda = \sigma_n\lambda$$

Thus, the nominal stress, σ_n can be expressed as:

$$\sigma_n = \frac{\sigma}{\lambda} = \sum_{r=1}^{n}\eta_r(\lambda^{\alpha_r-1} - \lambda^{-\frac{\alpha_r}{2}-1}) \tag{2-12}$$

where η_r has units of N/m^2 and α_r is dimensionless.

Usually, two terms in Eqn. 2-12 are good enough to describe the rubbery material behavior of uni-axial extension up to a stretch ratio of 7 [24]. A two-term Ogden's equation was adopted since the stretch ratio of this study is less than 2. Figure.2-2 is the comparison of Ogden's model with rubber force-elongation data given by Treloar [23].

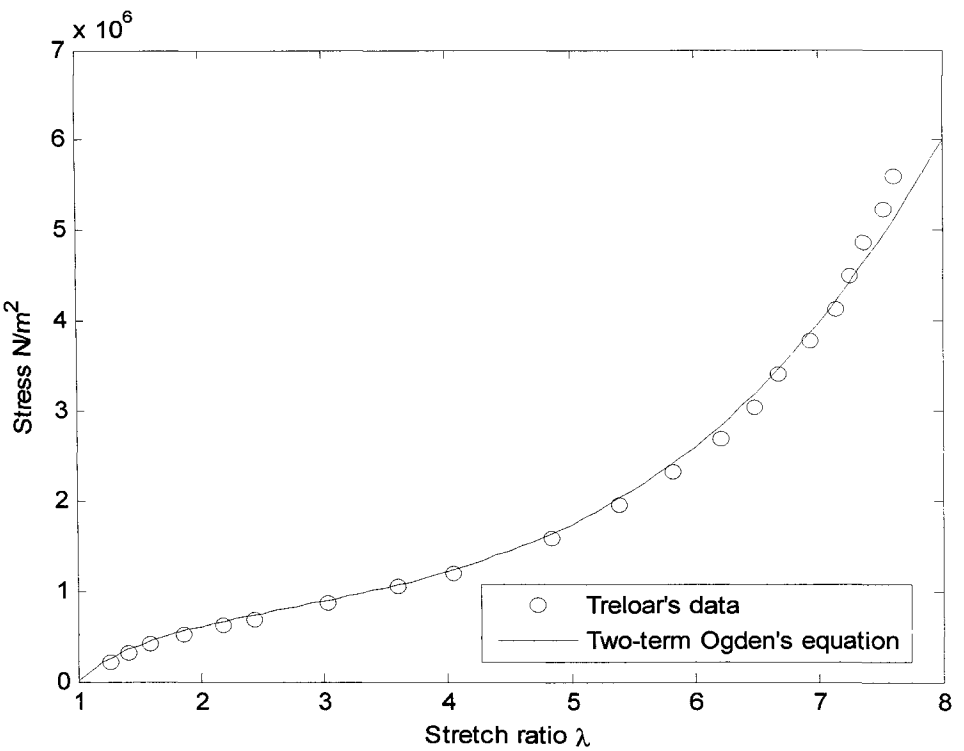

Fig. 2-2 The two-term Ogden's equation compared with Treloar's data in simple tension, with coefficients: $\eta_1 = 0.65MPa$, $\eta_2 = 1.18\times10^{-3}\ MPa$, $\alpha_1 = 1.3$ and $\alpha_2 = 5.0$.

2.4 Theory of Gas Sorption in Rubber with Deformation

The Flory-Huggins equation is capable of predicting gas sorption isotherms in rubbery polymers for stress-free states. However, if the rubber sample is deformed before being saturated with gas, the total Helmholtz free energy change will be different from a simple Flory-Huggins treatment.

Assuming that deformation and mixing are independent of each other, the total Helmholtz free energy change will be the sum of the free energy change due to mixing and deformation.

$$\Delta F = \Delta F_d + \Delta F_m \tag{2-13}$$

where ΔF_d and ΔF_m are changes of Helmholtz free energy of deformation and mixing respectively.

The Helmholtz free energy change due to mixing, ΔF_m can be obtained from Eqn. 2-7, while ΔF_d will be deduced from Ogden's model on rubber elasticity. By definition, the Helmholtz free energy change due to deformation is given by

$$dF_d = dU - d(TS) \tag{2-14}$$

And the energy change of deformation is

$$dU = TdS - PdV + V_0 \sigma d\lambda + \mu_2 dN_2$$

Where V_0 and V are the original volume and deformed volume, respectively. Substituting dU into Eqn.2-14, yields

$$dF_d = -PdV + V_0 \sigma d\lambda - SdT + \mu_2 dN_2$$

where V_0 is the volume of the undeformed sample, μ_2 is the rubber chemical potential, and N_2 is the number of rubber chains. With temperature constant, the third term on the

right hand side disappears. The number of rubber molecules is constant; thus, the last term on the right hand side is zero. The only contribution to the free energy is the work done on the rubber and PdV work due to dilation

$$dF_d = V_0 \sigma d\lambda - PdV \tag{2-15}$$

The change of Helmholtz free energy due to external work and dilation is obtained by

$$\Delta F_d = V_0 \int \sigma d\lambda - \int PdV \tag{2-16}$$

Since the rubber volume is quite small compared with the volume of the pressure vessel, and the amount of gas dissolved into the rubber is also small, the pressure during the gas absorption process can be treated as constant. And the work done from the dilation of rubbery sample is

$$\int PdV = P\Delta V \tag{2-17}$$

Before continuing calculating the Helmholtz free energy due to deformation, the relation between the stretch and gas concentration must be derived. This is necessary since the polymer will undergo dilation as gas is absorbed and this will affect the stretch ratio, λ. Stretch is defined as the ratio of the deformed length to the original length and dilation will alter the original length of the sample. This relates to the procedure used in the experiment where: 1) the rubber is stretched to a certain length; 2) the sample length is kept constant and is placed in a pressure vessel; 3) gas is introduced to a desired pressure level and equilibrium is established between the sample and gas.

The dimensions of the rubber sample at different stages in the process are shown in Fig. 2-3. L_{ox}, L_{0y} and L_{0z} are the undeformed dimensions of the rubber sample in X, Y, and Z-directions; L_{1x}, L_{1y} and L_{1z} are the dimensions after deformation; L_{2x}, L_{2y} and

L_{2z} are the final dimensions after equilibration with the gas. For the condition during the tests, L_{1x} is equal to L_{2x}, but that does not mean the stretch ratio is constant. The change in stretch ratio manifests itself as a change in force from f_0 to f_f as shown in Fig. 2-3.

Ideal rubber is an incompressible material with a Poison's ratio of 0.5 (Poison's ratio of silicone rubber and EPDM was measured to be 0.48; the detailed information is represented in Appendix. A). Thus, the volume of the sample after deformation is the same as the original volume:

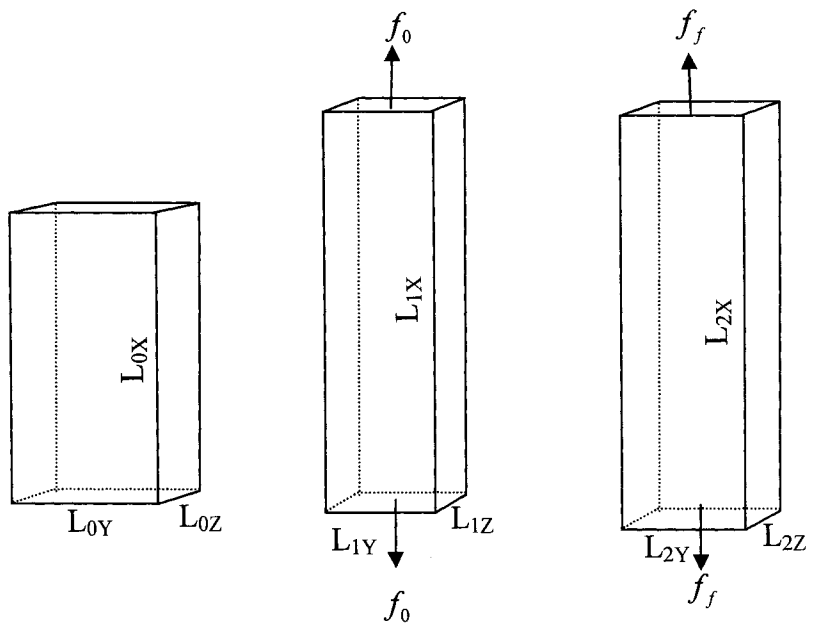

Fig. 2-3 Schematic of a rubber sample at different stages, (a) original sample, (b) deformed sample, (c) saturated sample with deformation. f_0 is the initial force, and f_f is the force after dilation.

$$V_0 = L_{0x}L_{0y}L_{0z} = L_{1x}L_{1y}L_{1z} = V_1$$

The volume after saturating with gas is given by

$$V_2 = L_{2x}L_{2y}L_{2z}$$

The volume dilation ratio of the rubber sample is defined as:

$$\Lambda = \frac{V_2}{V_1} = \frac{1}{\phi_2} = \frac{L_{2x}L_{2y}L_{2z}}{L_{1x}L_{1y}L_{1z}} = \frac{L_{1y}L_{1z}}{L_{2y}L_{2z}} \tag{2-18}$$

where L_{1x} and L_{2x} are equal to each other, and ϕ_2 is volume fraction of rubber.

Substituting Eqn. 2-18 into Eqn. 2-17 yields

$$\int PdV = PV_1\left(\frac{1}{\phi_2} - 1\right) = PV_0\left(\frac{1}{\phi_2} - 1\right) \tag{2-19}$$

For gas absorption in rubber, it has been shown [3, 7-10] that the dilation is isotropic, i.e. the linear dilation is the same in all dimensions. Although the length in X-direction is kept constant, the stretch ratio changes. The linear dilation ratio is defined as

$$\beta = \frac{L_{2y}}{L_{1y}} = \frac{L_{2z}}{L_{1z}}$$

Substituting β in Eqn. 2-18 leads to

$$\beta = \frac{1}{\sqrt{\phi_2}}$$

Since the dilation is isotropic, in X-direction the dilation ratio is also $\frac{1}{\sqrt{\phi_2}}$. Thus, instead of using L_{0x}, L_{0x}' was employed as the original length in X-direction to calculate the stretch ratio after dilation, where $L_{0x}' = \beta L_{0x}$. Thus, the stretch ratio, λ' in the final state in Fig. 2-3 is

$$\lambda' = \frac{L_{1x}}{L_{0x}'} = \frac{L_{1x}}{L_{0x} \times \beta} = \lambda\sqrt{\phi_2} \tag{2-20}$$

where $\lambda = \frac{L_{1x}}{L_{0x}}$ is the stretch ratio before exposing the rubber sample to gas. After dilation, the stress can be obtained by substituting λ' into Eqn. 2-12:

$$\sigma = \sum_{r=1}^{n} \eta_r (\lambda'^{\alpha_r - 1} - \lambda'^{-\frac{\alpha_r}{2} - 1})$$

$$= \sum_{r=1}^{n} \eta_r \left[\left(\lambda\sqrt{\phi_2}\right)^{\alpha_r - 1} - \left(\lambda\sqrt{\phi_2}\right)^{-\frac{\alpha_r}{2} - 1} \right] \tag{2-21}$$

The Helmholtz free energy change due to external force can be obtained by substituting Eqn. 2-21 into Eqn. 2-16,

$$\Delta F_d = \int V_0 \sigma d\lambda' - \int P dV$$

$$= \int V_0 \sum_{r=1}^{n} \eta_r \left[(\lambda\phi_2^{1/2})^{\alpha_r - 1} - (\lambda\phi_2^{1/2})^{-\frac{\alpha_r}{2} - 1} \right] d(\lambda\phi_2^{1/2}) - PV_0 \left(\frac{1}{\phi_2} - 1 \right)$$

$$= V_0 \sum_{r=1}^{n} \eta_r \left[\frac{1}{\alpha_r} (\lambda\phi_2^{1/2})^{\alpha_r} + \frac{2}{\alpha_r} (\lambda\phi_2^{1/2})^{-\frac{\alpha_r}{2}} - \frac{1}{\alpha_r} (\phi_2^{1/2})^{\alpha_r} - \frac{2}{\alpha_r} (\phi_2^{1/2})^{-\frac{\alpha_r}{2}} \right]$$

$$- PV_0 \left(\frac{1}{\phi_2} - 1 \right) \tag{2-22}$$

Differentiating ΔF_d with respect to N_1 yields

$$\left(\frac{\partial F_d}{\partial N_1} \right)_{N_2, T, L_{1x}, V_t} = \left(\frac{\partial F_d}{\partial \phi_2} \frac{\partial \phi_2}{\partial N_1} \right)_{N_2, T, L_{1x}, V_t}$$

$$= \frac{V_0}{2N_0} \sum_{r=1}^{n} \eta_r \left[\left(\lambda\phi_2^{1/2}\right)^{-\alpha_r/2} - \left(\lambda\phi_2^{1/2}\right)^{\alpha_r} - \left(\phi_2^{1/2}\right)^{-\alpha_r/2} + \left(\phi_2^{1/2}\right)^{\alpha_r} \right] + PV_0 \frac{\phi_2}{N_0} \tag{2-23}$$

where N_0 is the total number of the cells of the lattice, and $N_0 = N_1 + xN_2$, and the subscript V_t represents the total volume of the pressure vessel.

The Helmholtz free energy change due to mixing is given by Eqn. 2-7 and differentiating with respect to N_1 yields

$$\left(\frac{\partial \Delta F_m}{\partial N_1}\right)_{N_2,T,L_{1x},V_t} = kT\left[\ln(1-\phi_2) + (1-\frac{1}{x})\phi_2 + \chi\phi_2{}^2\right] \tag{2-24}$$

Normally, $1-\frac{1}{x} \approx 1$ because x is in the range of 10^3 and 10^4, or even higher, and Eqn. (2-24) becomes

$$\left(\frac{\partial \Delta F_m}{\partial N_1}\right)_{N_2,T,L_{1x},V_t} = kT\left[\ln(1-\phi_2) + \phi_2 + \chi\phi_2{}^2\right]$$

The total Helmholtz free energy was obtained by substituting Eqn. 2-7 and Eqn. 2-22 in to Eqn. 2-13. Differentiating the total Helmholtz free energy change with respect to N_1 yields the change of chemical potential of gas in the polymer,

$$\mu_1 - \mu_1{}^0 = \left(\frac{\partial \Delta F}{\partial N_1}\right)_{N_2,T,L_{1x},V_t} = \left(\frac{\partial \Delta F_m}{\partial N_1}\right)_{N_2,T,L_{1x},V_t} + \left(\frac{\partial \Delta F_d}{\partial N_1}\right)_{N_2,T,L_{1x},V_t}$$

$$= kT\left[\ln(1-\phi_2) + \phi_2 + \chi\phi_2{}^2\right] + \frac{V_0}{2N_0}\sum_{r=1}^{n}\eta_r\left[\left(\lambda\phi_2{}^{1/2}\right)^{-\alpha_r/2} - \left(\lambda\phi_2{}^{1/2}\right)^{\alpha_r} - \left(\phi_2{}^{1/2}\right)^{-\alpha_r/2} + \left(\phi_2{}^{1/2}\right)^{\alpha_r}\right]$$

$$+ PV_0\frac{\phi_2}{N_0} \tag{2-25}$$

At equilibrium, the chemical potential of the gas in the polymer must be equal to the chemical potential of the gas in the pure gas phase, i.e.

$$\left(\frac{\partial \Delta F / kT}{\partial N_1}\right)_{N_2,T,L_{1x},V_{t_t}} = \frac{\mu_1 - \mu_1{}^0}{kT} = \ln\frac{P}{P_0} \tag{2-26}$$

where μ_1 and $\mu_1{}^0$ are the chemical potential of the gas at pressure P and vapor pressure, P_0 is gas vapor pressure at temperature of the experiments. Substituting Eqn. 2-25 in Eqn.

2-26 yields

$$kT\ln\frac{P}{P_0} = kT\left[\ln(1-\phi_2)+\phi_2+\chi\phi_2^{\,2}\right] + \frac{V_0}{2N_0}\sum_{r=1}^{n}\eta_r\left[\left(\lambda\phi_2^{1/2}\right)^{-\alpha_r/2} - \left(\lambda\phi_2^{1/2}\right)^{\alpha_r} - \left(\phi_2^{1/2}\right)^{-\alpha_r/2} + \left(\phi_2^{1/2}\right)^{\alpha_r}\right] + PV_0\frac{\phi_2}{N_0} \qquad (2\text{-}27)$$

The quantity, N_0 is the total number of molecules and can be expressed as,

$$N_0 = \frac{N_1}{\phi_1} \qquad (2\text{-}28)$$

where N_1 is the number of gas molecules dissolved in rubber. This quantity can be obtained from the gas concentration in rubber as

$$N_1 = \frac{C[cm^3/cm^3]}{22410\left[\frac{cm^3}{mole}\right]} \times 6.022\times10^{23}\left[\frac{\#molecules}{mole}\right]$$

Substituting N_1 in Eqn. 2-28 yields

$$N_0 = \frac{C/22410}{\phi_1}\times 6.022\times10^{23}$$

The volume fraction of gas in the polymer, ϕ_1 is expressed as,

$$\phi_1 = \frac{N_1}{N_1 + xN_2} = \frac{CV_g/22410}{CV_g/22410+1} \qquad (2\text{-}29)$$

where V_g is the gas partial molar volume in rubber and is defined as,

$V_g = \left(\frac{\partial V_2}{\partial N_1}\right)_{T,N_2\ldots}$ (cm^3/mol), and can be obtained from rubber dilation measurements.

Substituting Eqn. 2-29 in Eqn. 2-28 yields

$$N_0 = \frac{\left(\frac{CV_g}{22410}+1\right)}{V_g} \times 6.022 \times 10^{23} \tag{2-30}$$

Substituting N_0 in Eqn. 2-27, the sorption isotherm is set up with two independent variables P and λ, which is the final model of gas sorption in rubber under stretch.

3. Measurement of Gas Absorption in Rubber with Deformation

3.1 Introduction

Over the past several decades, many techniques have been developed to measure the gas sorption isotherm in polymers, among which the most common methods are the barometric method and gravimetric method. The most popular barometric method relies on measurement of the pressure decay as gas is absorbed by the polymer [3, 7, 19-21]. The experiment is conducted by isolating a polymer sample and a high-pressure gas in a closed vessel. As the polymer absorbs the gas, the pressure drop in the vessel is monitored as a function of time. An equation of state for the gas is used to convert the pressure into the mass uptake in the polymer. Although it gives acceptable results, the dilation of the sample needs to be considered to obtain accurate measurement of the solute concentration.

For the gravimetric method, a microbalance or a quartz spring is employed in the test. Using a microbalance is a direct method to measure the gas sorption in polymers [8-14], which is based on measurement of the weight gained by a polymer sample when exposed to a gas. Some researchers used a sensitive quartz spring [16]; the method is based on the extension of a calibrated spring due to gas sorption. The increase in weight of the polymer sample, attached to the spring, is monitored with a cathetometer to accurately measure displacement. The disadvantages of the gravimetric methods are that there are uncertainties due to the buoyancy correction. At relatively high pressures, the polymer sample dilates due to sorption of gas, which generates an additional buoyancy force that needs to be taken into account.

The gravimetric method was adopted in this study since it gives a direct

measurement of weight gain. Instead of measuring weight gain of the sample, the weight loss is measured after the polymer sample has equilibrated with the gas. The sample is removed from the pressure vessel and placed on a micro-balance to measure weight loss. This technique was used because the polymer sample must be stretched using a rigid metal frame. The total weight of the frame and sample would be too large to use with a quartz spring which has a small load range.

3.2 Rubbery Polymer Samples

The polymer samples used in the tests were silicone rubber and ethylene propylene diene monomer (EPDM). The samples were manufactured as rubber bands in order that these samples could be stretched uniformly to a desired level, from stretch ratio of 1(no stretch) to 1.9.

The silicone rubber is a commercial product supplied by Aero Rubber Company Inc, Bridgeview, Illinois, USA, as a rubber band. The dimensions are approximately 124.8 *mm* in length (perimeter), 3.9 *mm* in width and 0.3 *mm* in thickness. The sample weight is approximately 0.2 *gram* ; and the density is measured to be $1.22 \pm 0.08\ g/cm^3$ (weight divided by volume). The degree of crystallinity was determined to be zero using a differential scanning calorimetry (DSC) (see Appendix B for details). The zero degree of crystallinity allowed us to adopt Ogden's model for rubber elasticity, since the model assumes the rubber is homogeneous and isotropic in undeformed state.

The EPDM is a commercial product supplied by AERO RUBBER COMPANY INC, as a rubber band. The dimensions are approximately 143.6 *mm* in length (perimeter), 6.6 *mm* in width and 1.0 *mm* in thickness. The weight is approximately 0.9 *gram* , and the density is $1.08 \pm 0.02\ g/cm^3$. EPDM is known to have nearly zero

degree of crystallinity [35, 36].

The carbon dioxide used in this study was obtained from Praxair Canada Inc. The carbon dioxide has a purity at least 99.99%. The gas was used as-received without any treatment.

3.3 Test Methodology

The samples were first placed in a pressure vessel with dimensions (outer diameter: 60mm, inner diameter: 40mm, and length: 290mm) that allows the rubber samples be stretched up to stretch ratio of 1.9 and exposed to carbon dioxide gas at pressures up to 1.72 *MPa* . The pressure was measured with a Validyne DP15-20 pressure transducer with a voltage resolution of 0.1 *mv* , which provides a resolution of 138 *Pa* for pressure measurement. Since there was no active temperature control, the temperature during the test was kept at a room temperature of approximately 20°C with a temperature variation of ± 0.5°C during the test period. The samples were allowed to equilibrate with CO_2 for approximately 1 hour (the time needed to reach equilibrium will be discussed later on). After equilibrium had been reached, the pressure vessel was decompressed; the samples were quickly removed from the vessel and placed on an analytical balance (Denver Instrument M-120) with a weight resolution of 0.1 *mg* . The weight change of the sample was recorded as a function of time. The microbalance is sensitive to temperature changes and in order to keep the surrounding temperature of the microbalance constant, the microbalance was placed inside an environmental chamber and set to a temperature of 20°C with a variation range of ± 0.1°C.

Initially, there was a delay of approximately 20 seconds in recording weight change while the sample was removed from the pressure vessel and placed on the

analytical balance. There is a 13% to 19% loss of mass in CO_2 gas from the sample for the tested pressure range during this initial delay time and this must be accounted for in some way in order to measure the value of solubility accurately.

In order to make this correction, diffusion theory [22] was employed to predict the desorption process based on a diffusion model in an infinitely thin sheet with an initial concentration C_0, as shown in Fig.3-1. Since the dimensions of the silicone rubber and EPDM are $125 \times 4 \times 0.3mm$ and $144 \times 6.6 \times 1mm$ respectively, the thickness is rather small compared to the length and width; thus the edge surfaces are negligible compared with the plane surface. Thus, it is reasonable to treat the rubber sample as a plane sheet, which means the diffusing substance diffusing out through the edges is negligible. Therefore, it is assumed that all the diffusion occurs through the plane surfaces.

The theory assumes that the diffusion coefficient D is independent of concentration for dilute solutions, and the material is isotropic. With an initial uniform concentration C_0 throughout the plane sheet, and the surfaces kept at a constant concentration C_1, the solution to the diffusion equation is,

$$\frac{C - C_0}{C_1 - C_0} = 1 - \frac{4}{\pi} \sum_{n=0}^{\infty} \frac{(-1)^n}{2n+1} e^{-D(2n+1)^2 \pi^2 t / 4l^2} \cos \frac{(2n+1)\pi x}{2l} \quad (n = 1,\ 2, 3 \cdots) \qquad (3\text{-}1)$$

where C is gas concentration in the sample, D is diffusion coefficient in unit of $m^2 \cdot \sec^{-1}$, t is time in second, x is the coordinate in X-direction as shown in Fig.3-1, and l is the half thickness of the plane sheet.

The desorption tests were carried out at atmospheric pressure in the current study. Assuming that desorption is dominated by diffusion and not by convection at the surface, and neglecting CO_2 concentration in atmosphere (CO_2 concentration in air is 0.036%),

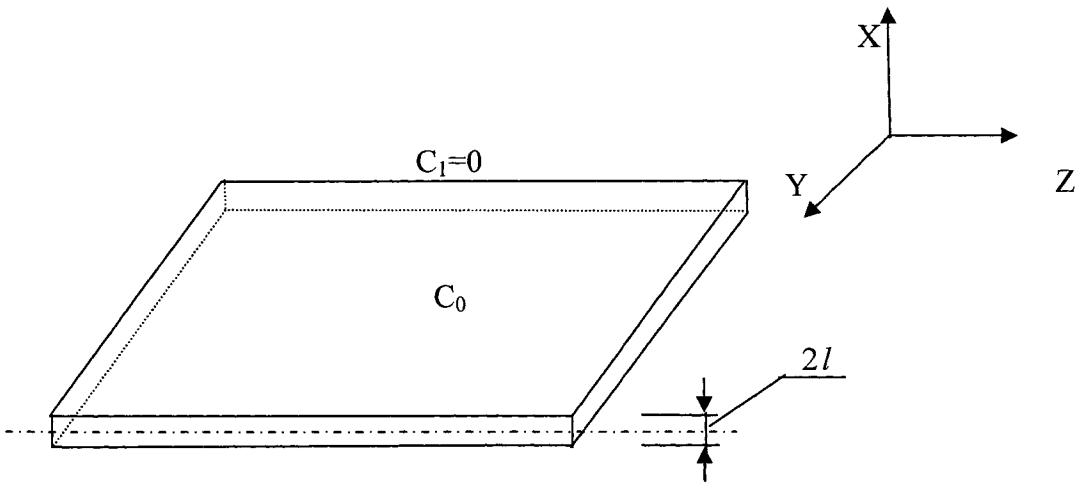

Fig. 3-1 Infinitely thin sheet with an initial uniform concentration. The coordinate origin is located at the geometric center of the plane sheet.

C_1 can be reasonably assumed to be zero. Substituting $C_1 = 0$ into Eqn. 3-1 yields

$$C = \frac{4C_0}{\pi}\sum_{n=0}^{\infty}\frac{(-1)^n}{2n+1}e^{-D(2n+1)^2\pi^2 t/4l^2}\cos\frac{(2n+1)\pi x}{2l} \tag{3-2}$$

The total mass of gas remaining in the rubber band at time t is obtained by integrating Eqn 3-2 over the volume of the sample.

$$m_t = A\int_{-l}^{l} C dx = A\frac{16C_0 l}{\pi^2}\sum_{n=0}^{\infty}\left\{\frac{1}{(2n+1)^2}e^{-D(2n+1)^2\pi^2 t/4l^2}\right\} \tag{3-3}$$

where A is area of one side of the plane sheet of the sample.

A least square method was used to fit Eqn. 3-3 to the measured mass decay curve in order to determine D and C_0. Since Eqn. 3-3 is in series form, the number of terms needed to describe the desorption phenomenon must be determined. A five-term equation was used first, and then compared with the fit for a four-term equation. If both of the results are comparable, a three-term equation was used; otherwise a six-term equation

was used. For the five-term equation, m_t was expressed as

$$m_t = k_1 C_o [e^{-k_2^2 Dt} + \frac{1}{9} e^{-9k_2^2 Dt} + \frac{1}{25} e^{-25k_2^2 Dt} + \frac{1}{49} e^{-49k_2^2 Dt} + \frac{1}{81} e^{-81k_2^2 Dt}]$$

where $k_1 = \frac{16}{\pi^2} Al$ and $k_2 = \frac{\pi}{2l}$. Define the square of the error as

$$E^2 = \sum_{i=1}^{N} \left\{ m_i - k_1 C_o [e^{-k_2^2 Dt_i} + \frac{1}{9} e^{-9k_2^2 Dt_i} + \frac{1}{25} e^{-25k_2^2 Dt_i} + \frac{1}{49} e^{-49k_2^2 Dt_i} + \frac{1}{81} e^{-81k_2^2 Dt_i}] \right\}^2 \quad (3\text{-}4)$$

where m_i is the measured mass of gas remaining in the sample at a certain time t_i, which is obtained by subtracting the mass of the sample from the reading of the balance since the reading includes both the mass of the sample and sorbed gas, and N is the number of data points. Taking partial derivative of Eqn. 3-4 with respect to D and C_0 respectively yields two equations with two unknowns D and C_0. In order to find D and C_0 that give minimum square error, the two equations must be solved:

$$\left.\frac{\partial E^2}{\partial C_o}\right|_D = 0 \text{ and } \left.\frac{\partial E^2}{\partial D}\right|_{C_0} = 0$$

The first equation yields C_0 to be

$$C_o = \frac{\sum_{i=1}^{N} m_i \left[e^{-k_2^2 Dt_i} + \frac{1}{9} e^{-9k_2^2 Dt_i} + \frac{1}{25} e^{-25k_2^2 Dt_i} + \frac{1}{49} e^{-49k_2^2 Dt_i} + \frac{1}{81} e^{-81k_2^2 Dt_i} \right]}{k_1 \sum_{i=1}^{N} \left[e^{-k_2^2 Dt_i} + \frac{1}{9} e^{-9k_2^2 Dt_i} + \frac{1}{25} e^{-25k_2^2 Dt_i} + \frac{1}{49} e^{-49k_2^2 Dt_i} + \frac{1}{81} e^{-81k_2^2 Dt_i} \right]^2} \quad (3\text{-}5)$$

and the second equation leads to

$$\left.\frac{\partial E^2}{\partial D}\right|_{C_0} = \sum_{i=1}^{n} m_i t_i \left[e^{-k_2^2 Dt_i} + e^{-9k_2^2 Dt_i} + e^{-25k_2^2 Dt_i} + e^{-49k_2^2 Dt_i} + e^{-81k_2^2 Dt_i} \right] -$$

$$k_1 C_o \sum_{i=1}^{n} t_i \left[e^{-k_2^2 Dt_i} + \frac{1}{9} e^{-9k_2^2 Dt_i} + \frac{1}{25} e^{-25k_2^2 Dt_i} + \frac{1}{49} e^{-49k_2^2 Dt_i} + \frac{1}{81} e^{-81k_2^2 Dt_i} \right] \times$$

$$[e^{-k_2^2 Dt_i} + e^{-9k_2^2 Dt_i} + e^{-25k_2^2 Dt_i} + e^{-49k_2^2 Dt_i} + e^{-49k_2^2 Dt_i}] = 0 \quad (3\text{-}6)$$

In order to simplify Eqns. 3-5 and 3-6, A_i and B_i are defined as

$$A_i = e^{-k_2^2 Dt_i} + \frac{1}{9}e^{-9k_2^2 Dt_i} + \frac{1}{25}e^{-25k_2^2 Dt_i} + \frac{1}{49}e^{-49k_2^2 Dt_i} + \frac{1}{81}e^{-81k_2^2 Dt_i}$$

and

$$B_i = e^{-k_2^2 Dt_i} + e^{-9k_2^2 Dt_i} + e^{-25k_2^2 Dt_i} + e^{-49k_2^2 Dt_i} + e^{-81k_2^2 Dt_i}$$

Substituting A_i and B_i in Eqn 3-5 yields

$$C_o = \frac{\sum_{i=1}^{n} m_i A_i}{k_1 \sum_{i=1}^{n} A_i^2} \quad (3\text{-}7)$$

Substituting Eqn. 3-7 in Eqn. 3-6 yields

$$\sum_{i=1}^{n} m_i t_i B_i - k_1 \frac{\sum_{i=1}^{n}(m_i A_i)\sum_{i=1}^{n}(t_i A_i B_i)}{k_1 \sum_{i=1}^{n}(A_i^2)} = 0 \quad (3\text{-}8)$$

where the only unknown is D. The method of bisection [29] was used to solve for D with a lower limit $1\times10^{-5}\ cm^2\ \sec^{-1}$ and a higher limit $1\times10^{-9}\ cm^2\ \sec^{-1}$ for both silicone rubber and EPDM. Finally, C_0 is obtained by substituting D in Eqn. 3-5.

Figure 3-2 shows a typical CO_2 gas desorption process in silicone rubber. By examining Fig. 3-2, many plateaus were found where m_t was constant with time. However, the mass of gas remaining in the rubber band should decrease continuously until there is no gas left in the rubber sample. Therefore, it is believed that the plateaus are due to the limit of resolution of the analytical balance ($\pm$ 0.1mg). To avoid errors caused by the resolution limit, the least square fit only used the first data point on each

plateau. The selected data are shown in Fig. 3-3. A desorption curve based on a five-term diffusion model is also shown in Fig. 3-3 for comparison. From Fig. 3-3 it can be seen that the CO_2-rubber desorption phenomenon is described accurately by the diffusion model.

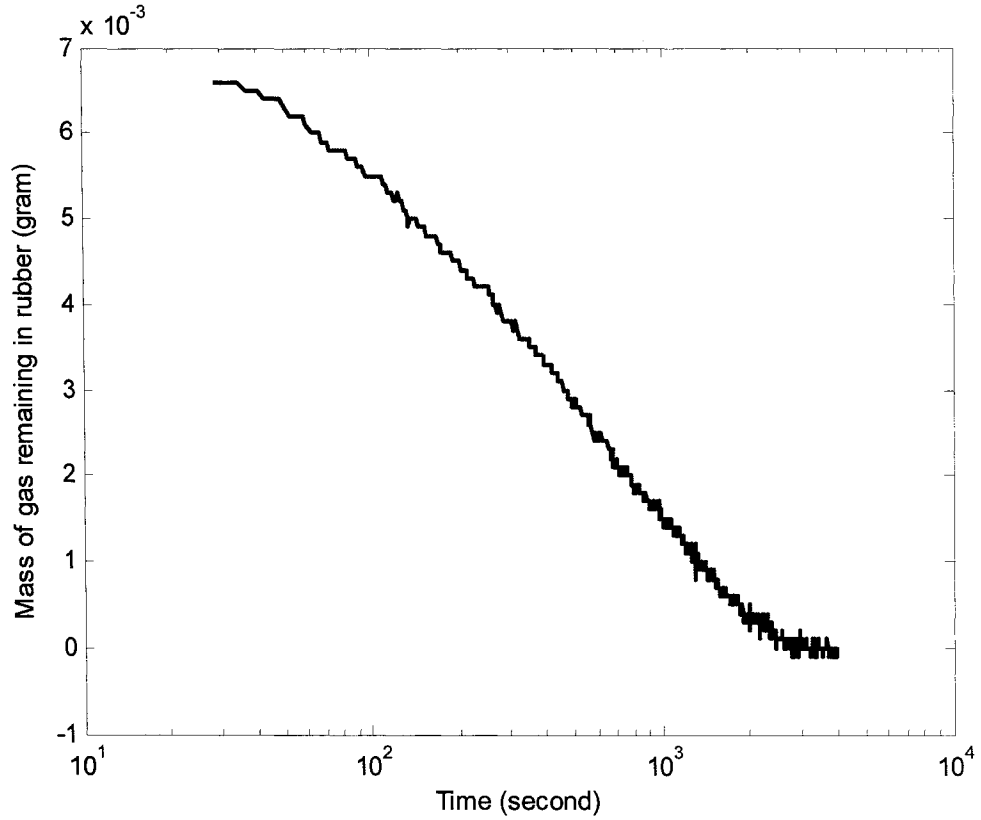

Fig.3-2 A typical CO_2 gas desorption curve in silicone rubber at $20^{o}C$, after equilibrating with CO_2 at1.72 *MPa* and under a stretch ratio of 1.9.

A two-, three- and four-term Eqn. 3-3 could be solved using the same method as presented previously. Comparing the results of the two-term, three-term, four-term and five-term equations (as shown in Table 3-1), it was found a four-term equation was good enough to describe the CO_2-rubber desorption phenomenon, and hereafter, a four-term equation was employed.

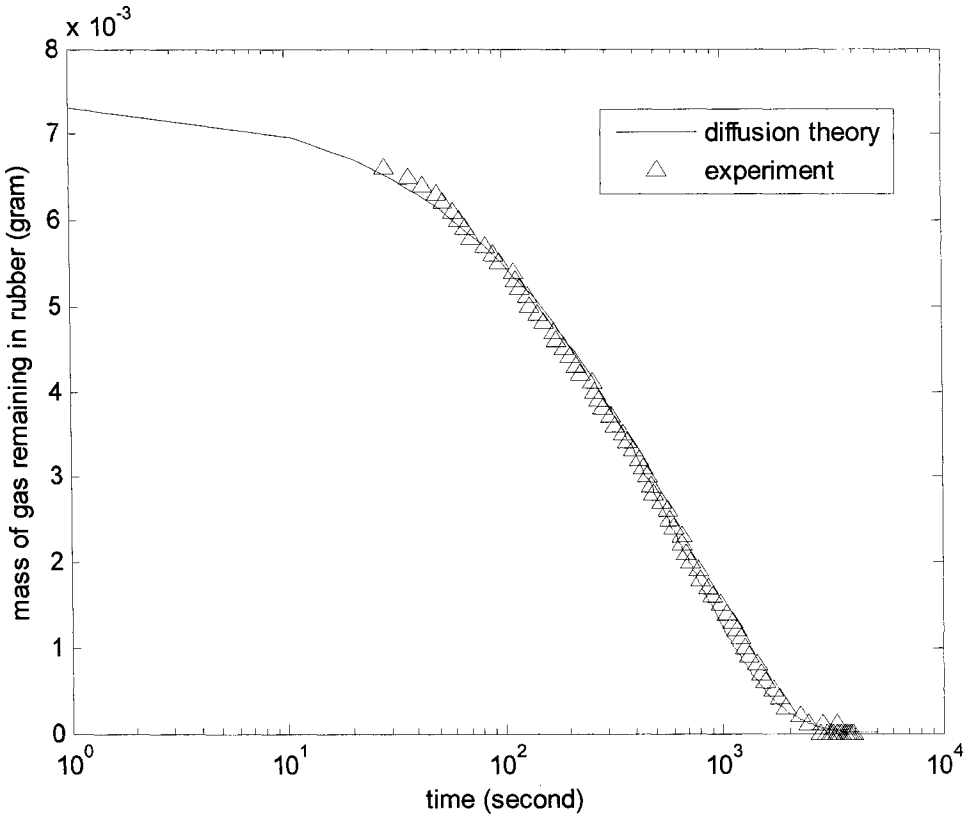

Fig. 3-3 A typical CO_2 -silicone rubber desorption curve compared with selected experimental data at 20°C, after equilibrating with CO_2 at 1.72 *MPa* and under a stretch ratio of 1.9.

Table. 3-1 D and C_0 obtained from two-term, three-term, four-term and five-term Eqn. 3-3

	2-term	3-term	4-term	5-term
C_0 cm^3 gas(STP)/cm^3 rubber	26.19	26.07	26.00	26.00
D cm^2sec^{-1}	1.48E-7	1.47E-7	1.47E-7	1.47E-7

Reexamining Fig.3-3, it was found that the desorption process for the silicone rubber and pressure of 1.72 *MPa* was completed within an hour, (the test shown in Fig. 3-3 was finished at around 2600 seconds or less than 44 minutes). So an hour should be sufficient to complete a sorption test. In order to determine the time needed for gas

sorption in rubber band to reach equilibrium, tests with 5 hours and 1 hour saturation times were carried out for silicone rubber and EPDM at stretch from1 to 1.9. The tests results are shown in Table.3-2. It was found that 1 hour is long enough for sorption of carbon dioxide in the rubber samples to reach equilibrium for pressures up to 1.72MPa. Thus for all the tests, the samples were allowed to equilibrate with CO_2 for 1 hour.

Table. 3-2 CO_2 concentrations in rubbers (silicone rubber and EPDM) of 5 hours and 1 hour saturation at pressure of 1.72 *MPa* in unit of [cm^3 gas (STP)/cm^3 rubber]

		1 hour	5 hour
Silicone rubber	Stretch=1	25.44	25.50
	Stretch=1.9	25.88	25.88
EPDM	Stretch=1	11.80	11.80
	Stretch=1.9	11.85	11.85

3.4 Gas Sorption Measurement in Rubber with Uni-directional Stretch

Since uni-directional extension is easy to generate, and the purpose of this study is to verify the effect of stretch on gas sorption in rubber, it is not necessary to cover all kinds of deformation; only uni-directional extension was considered in this study.

To measure the gas sorption in rubber with uni-directional stretch, the rubber sample needs to be stretched to a desired level and held in place to reach equilibrium with the gas. The schematic of the device used to hold the rubber sample is shown in Fig. 3-4 (the dimensions of the frame is given in Appendix. C). The frame was made up of an aluminum bracket. In the middle of the main post, there are four strain gages arranged in a full bridge. Two bearings were attached to each end of the frame and the rubber sample was stretched over the two bearings. The distance between the two bearings is adjustable so that the stretch ratio of the rubber band can be varied from 1 to 1.9.

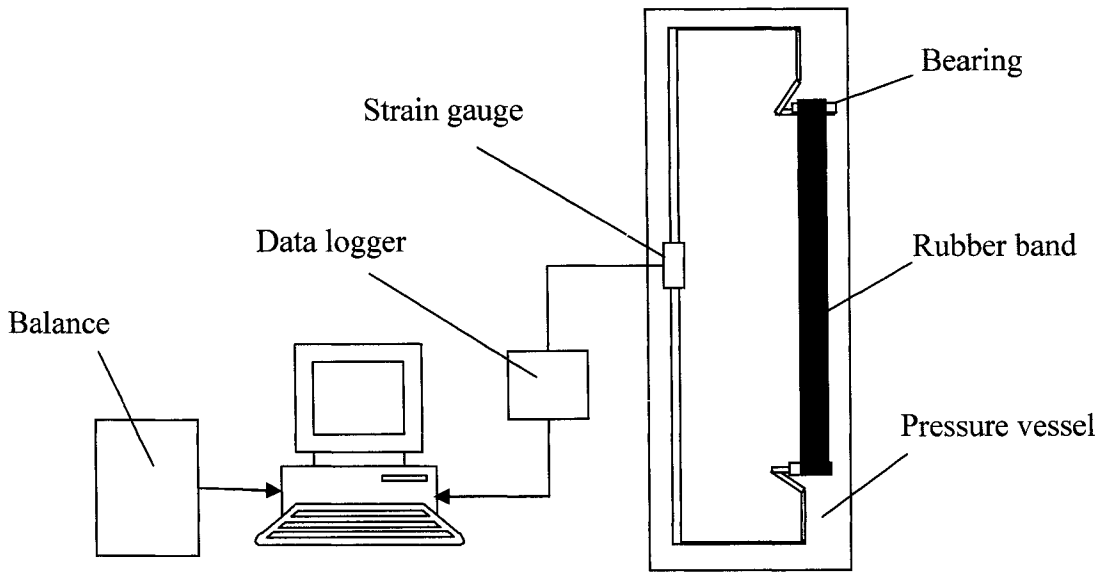

Fig.3-4 Schematic of test equipment used for gas sorption in rubber under stretch

The test procedure involved the following steps: stretch the rubber band to a desired level, hold it on the two bearings and rotate those two bearings in order to make sure the tension is uniform throughout the sample. The frame was placed in the pressure vessel and gas was introduced into the pressure vessel to a given pressure. The sample was then allowed to equilibrate with gas for one hour.

The output of the strain gauge bridge was sent to a computer through a data-logger as a function of time. For a given stretch, the stress decreases as a function of time and this is known as stress relaxation. The first one-hour stress relaxation data of silicone rubber and EPDM are plotted in Fig. 3-5 and Fig. 3-7, respectively. During the initial phase of the equilibration (< 100 seconds), there was a transient increase of stress in the rubber sample above the stress corresponding to the sample in air. This was caused by the initial temperature transient that occurred when CO_2 gas was rapidly introduced into the pressure vessel. However, after the transient period, lower stresses at 1.72 *MPa* were

observed than for the sample in air. The decrease in stress below the values corresponding to air is a direct result of the reduction in stretch ratio in the X-direction (direction of the applied load). Although the length in the X-direction L_{1x} is fixed, the reference length L_{0x} changes due to dilation from the absorption CO_2 gas. This decrease in λ causes a decrease in stress (refer to the discussion associated with Fig. 2-3).

Towards the end of the equilibration period (approximately 1 hour), the dilation effect on stress stopped but there remained a steady decrease in stress due to relaxation of the rubber sample. From the measurement, the residual relaxation rates are approximately the same for the rubber sample in air and in CO_2 as shown in Fig. 3-5 and Fig. 3-7 for silicone rubber and EPDM respectively. The difference of the stress relaxation between at atmospheric pressure and at 1.72 MPa tends to converge to a constant value, as shown in Fig. 3-6 and Fig. 3-8 for silicone rubber and EPDM respectively. Overall, the total decrease in stress over a 1 hour period, due to dilation and relaxation is only about 10%. Stress relaxation is not included in the model for predicting the effect of stretch on solubility because stress relaxation is a non-equilibrium effect. The model is based on the thermodynamic equilibrium between pure gas and rubber at constant stress.

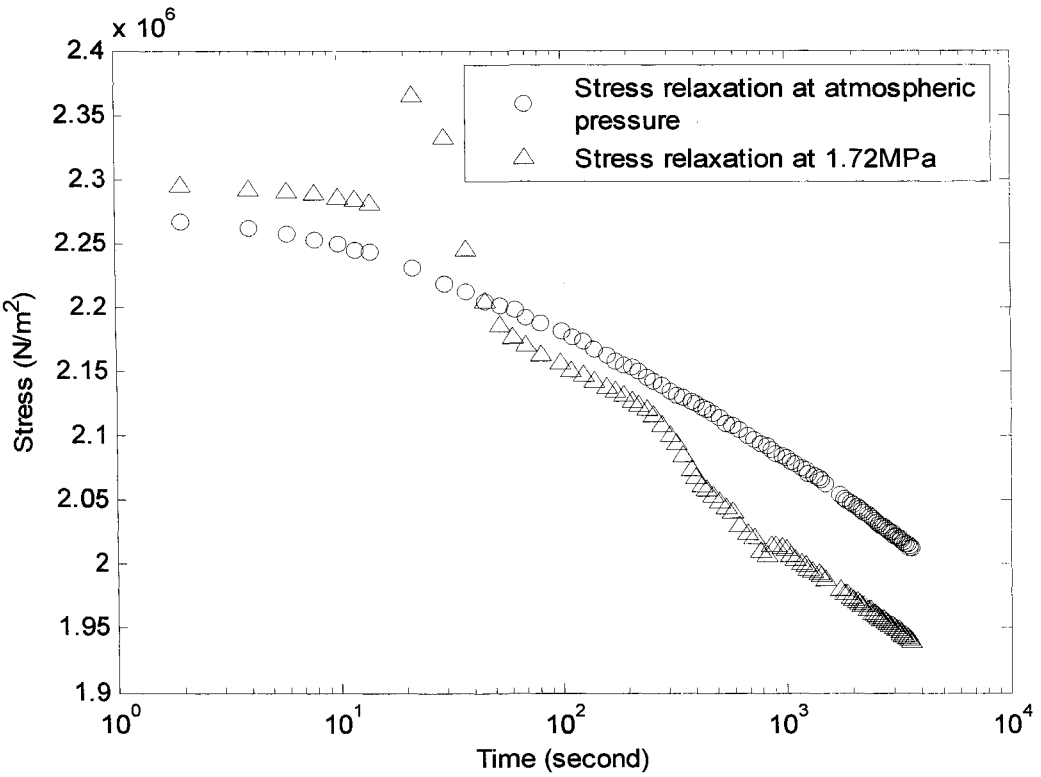

Fig. 3-5 Stress relaxations in silicone rubber at atmospheric condition and a CO_2 pressure of 1.72 *MPa*

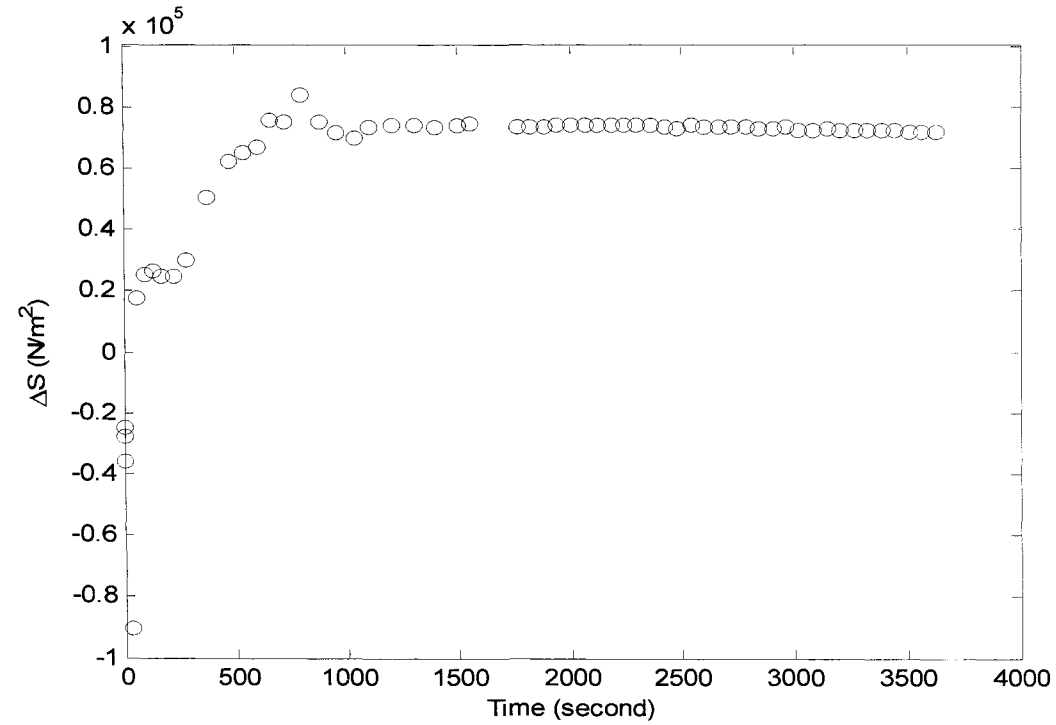

Fig. 3-6 Difference of silicone rubber stress relaxation between at atmospheric pressure and at 1.72 *MPa*

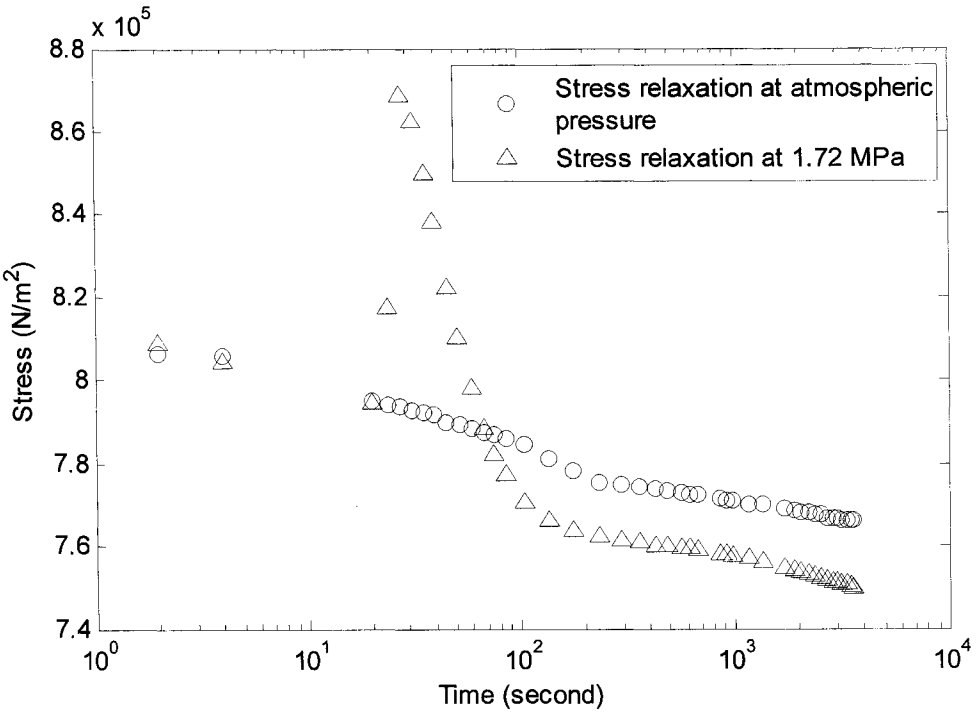

Fig. 3-7 Stress relaxations in EPDM at atmospheric pressure and a CO_2 pressure of 1.72 *MPa*

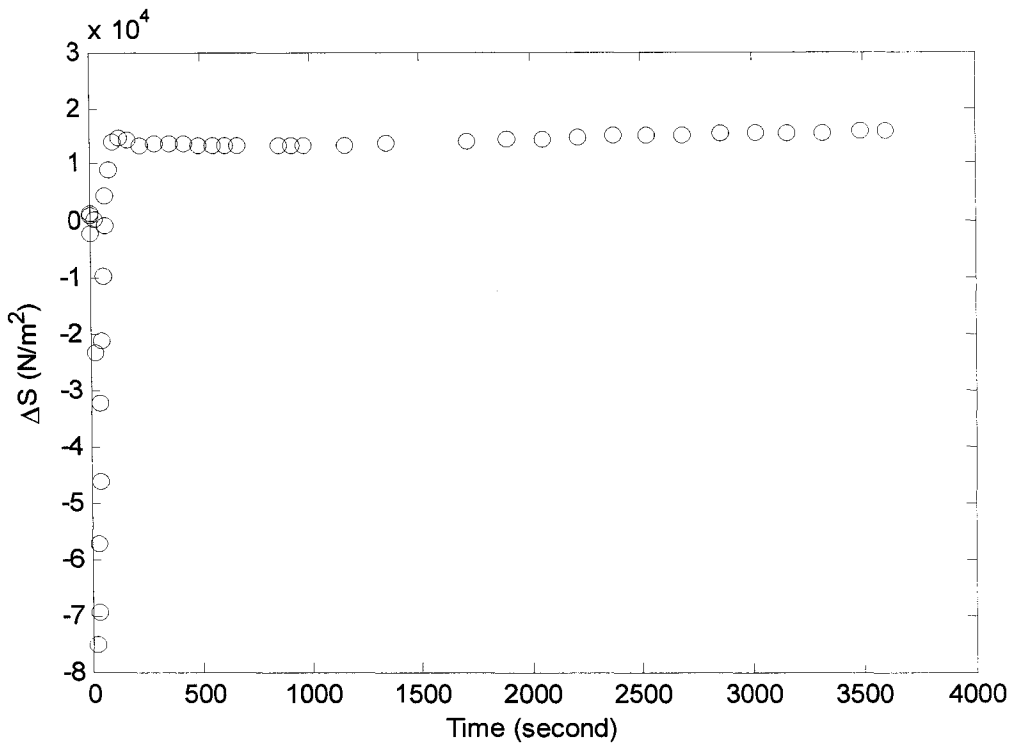

Fig. 3-8 Difference of EPDM stress relaxation between at atmospheric pressure and at 1.72 *MPa*

3.5 Dilation Measurement

A microscope combined with a digital camera (Nikon D70) was used to measure the dilation of the rubber sample with uni-axial deformation under high pressure. The pressure vessel used in the test is of the same size and shape as used in the CO_2 sorption tests but was modified with two windows as shown in Fig. 3-9, so that the rubber sample inside the vessel could be viewed through a microscope.

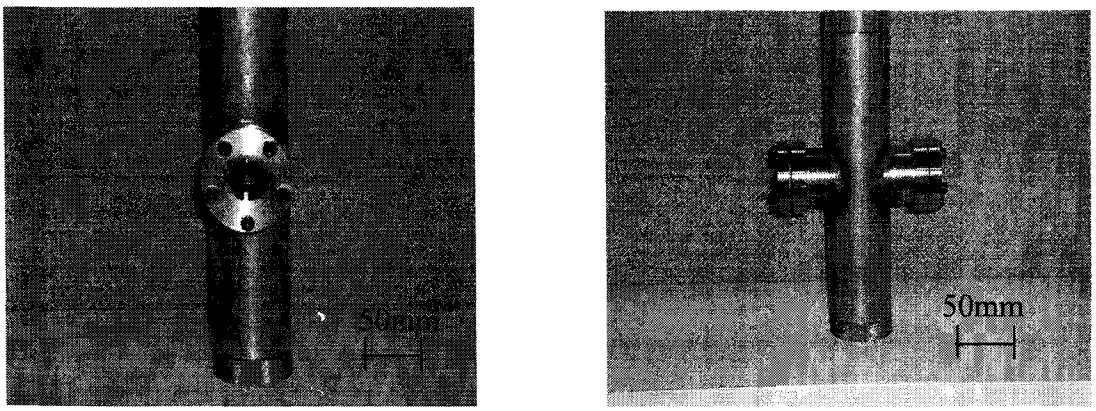

(a) **(b)**

Fig. 3-9 Photographs of pressure chamber used for measuring the rubber dilation: (a) front view, (b) side view.

A schematic of the device holding the rubber band is shown in Fig.3-10. A reference ruler was attached to the frame so the width of the rubber could be measured directly. To measure the dilation of the rubber sample when exposed to CO_2 at elevated pressure, the rubber band was stretched and held at constant length. A picture was taken after putting the frame and rubber sample into the pressure vessel. The vessel was pressurized with CO_2 at a given pressure and the sample was allowed to equilibrate for 1 hour. After equilibration, a photograph was taken showing the width of the sample. The pressure was increased in steps of about 0.4 *MPa* up to 1.72 *MPa* and photographs were taken at each pressure.

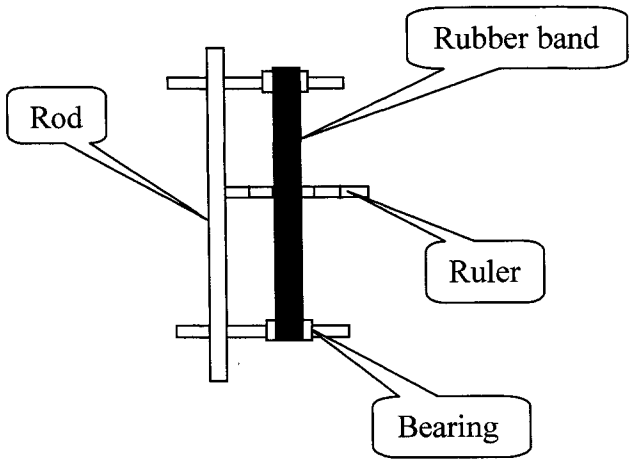

Fig.3-10 Schematic of the frame that holds the rubber band for dilation measurement

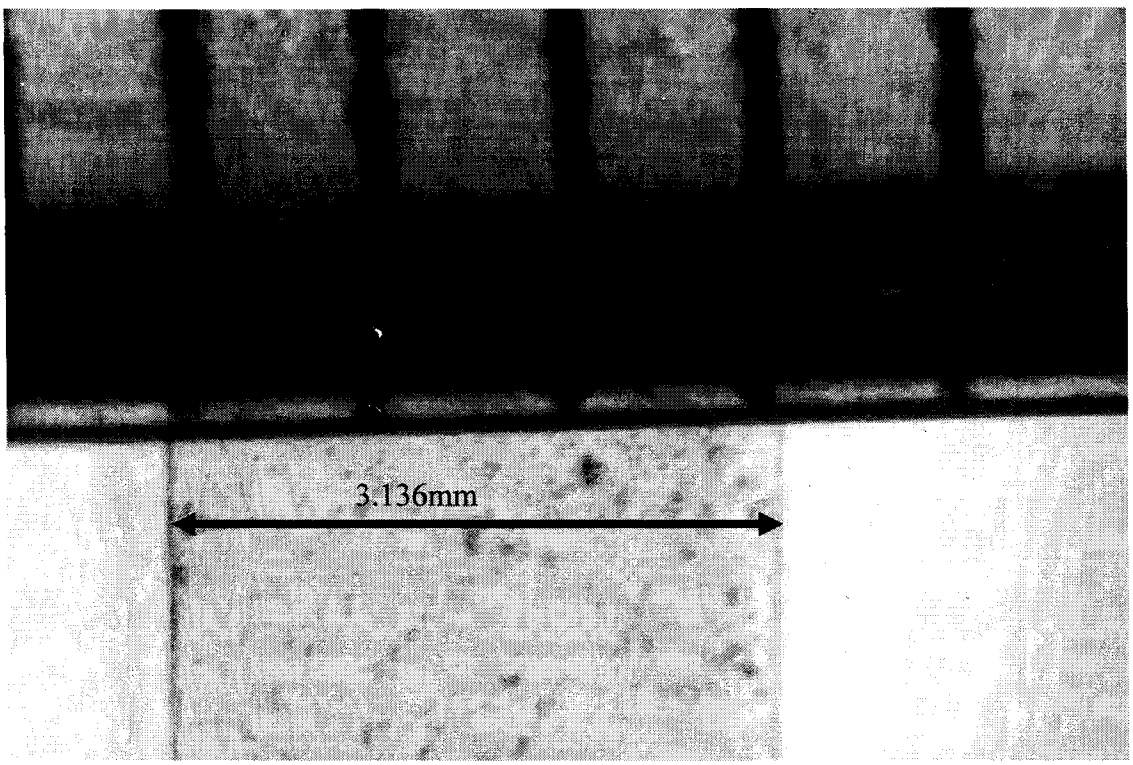

Fig. 3-11 A typical picture of rubber dilation measurement

Photoshop® was used to edit the picture and measure the width dilation of the rubber band upon absorbing CO_2 gas. Opening the picture with Photoshop®, an image

like Fig. 3-11 appears. Placing the cursor at both edges of the rubber band, the coordinates in units of pixels of the points will be shown at the top right of the screen. With the coordinates at hand, the width of the rubber sample can be obtained directly. Typically, the image of the rubber band width of 3mm corresponded to 1100 pixels and the accuracy of the measurement was 0.3%. Since for each sample, there are 5 photos taken at different pressure levels, it is important to measure the same position every time in case the width of the sample is not uniform. The only linear dilation measurement was for the width of the rubber sample. It was assumed that the linear dilation in the other two directions were the same based on isotropic dilation.

4. Results and Discussion

4.1 Introduction

The theory of gas sorption in rubber with uni-axial deformation was fully expanded in Section. 2, but it is not convincing without experimental support. In this section, the parameters of Ogden's equation of rubber elasticity will be determined in order to calculate the Helmholtz free energy change due to deformation. The gas sorption test results will also be presented. In order to fit the Flory-Huggins theory with experimental results, the partial molar volume, vapor pressure of CO_2 and the Flory-Huggins parameter must be obtained, and the procedure will be discussed. The thermodynamic model developed in Section.2 will be compared with experimental data.

4.2 Coefficients in Ogden's Equation

Ogden's equation has been proven to give a good prediction of the stress-stretch relationship for rubbers [23, 24]. Since for a two-term equation there are four coefficients, the key point is how to determine the coefficients. A two-term Ogden's equation is given as

$$\sigma_n = \eta_1(\lambda^{\alpha_1-1} - \lambda^{-\alpha_1/2-1}) + \eta_2(\lambda^{\alpha_2-1} - \lambda^{-\alpha_2/2-1}) \tag{4-1}$$

where σ_n is the nominal stress based on the area of the undeformed cross-section of the rubber sample, η_i and α_i, $i = 1,2$, are coefficients to be determined, and λ is stretch ratio. According to Ogden, the first term dominates the series in the low stretch range, $1 < \lambda < 1.8$. Thus, only the first term of Eqn. 4-1 was considered for the low stretch ratios. A single-term equation is given as

$$\sigma_n = \eta_1(\lambda^{\alpha_1-1} - \lambda^{-\alpha_1/2-1}) \tag{4-2}$$

Examining the rubber stress-stretch data shown in Fig.4-1, the initial part of the stress-stretch curve (up to stretch of 1.18) is in an approximately linear relationship. The slope of the initial part was found to be 5.75 *MPa* and the intercept on the stress axis was -5.72 *MPa* .

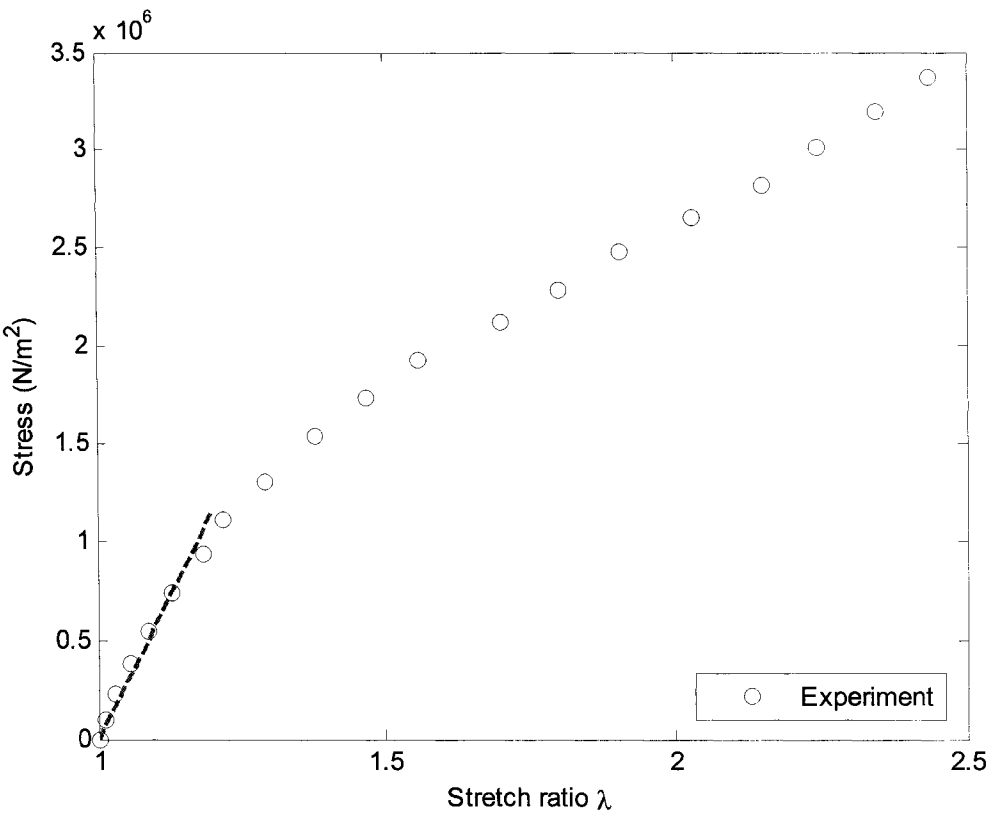

Fig. 4-1 The silicone rubber stress-stretch curve at 20°C

Thus, the stress-stretch relationship for the initial part is approximately given as

$$\sigma_n = 575\lambda - 572 \approx 575(\lambda - 1) \tag{4-3}$$

If η_1 was determined to be 575 N/cm^2, $(\lambda - 1)$ must be equal to $\left(\lambda^{\alpha_1 - 1} - \lambda^{-\alpha_1/2-1}\right)$ for the low stretch range. For the low stretches, a number of α_1 values were obtained by equating Eqns. 4-2 and 4-3 to be Eqn 4-4 that was solved for α_1, at different values of λ in the low stretch range and the results are given in Table 4-1,

$$\lambda - 1 = \lambda^{\alpha_1 - 1} - \lambda^{-\alpha_1/2 - 1} \tag{4-4}$$

Table. 4-1 The calculated value of α_1 in the small stretch range.

Stretch ratio	1.01	1.030	1.058	1.086	1.128	1.183	Average value
α_1	0.68	0.69	0.72	0.74	0.78	0.83	0.74

The single term Ogden's equation with coefficients, $\eta_1 = 5.75MPa$ and $\alpha_1 = 0.74$ is plotted in Fig.4-2 and compared with experimental data.

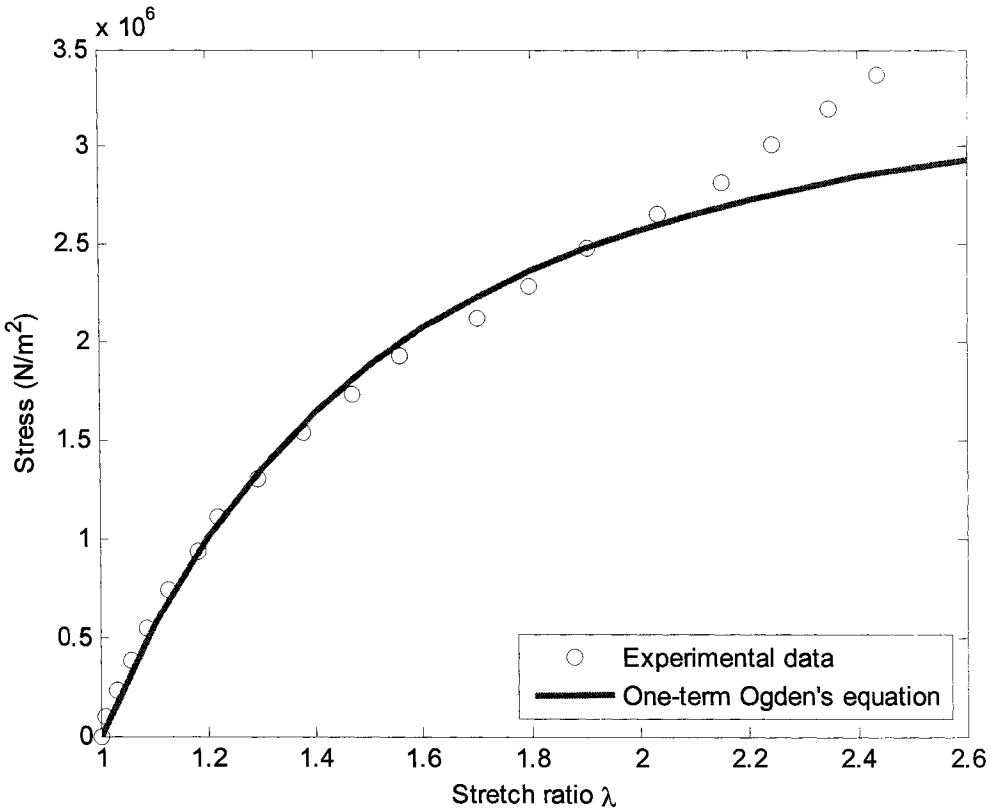

Fig.4-2 One term Ogden's equation with $\eta_1 = 5.75MPa$ and $\alpha_1 = 0.74$ compared with experimental data for silicone rubber.

Examining Fig. 4-2, slight differences between the equation and experimental data above stretch ratio 1.5 were found. In order to minimize the error to get a better fit, a least

squares fit was used to find a better value of η_1. The square of the error is defined as

$$E^2 = \sum_{i=1}^{n} (y_i - \sigma^1{}_i)^2$$

where y_i is the measured nominal stress at a certain stretch, $\lambda \leq 2.0$, since good fit up to stretch ratio of about 2.0 was achieved as shown in Fig. 4-2, and $\sigma^1{}_i$ is the single term Ogden's equation prediction. For $\alpha_1 = 0.74$, the value of η_1 that yields the least square error can be obtained by solving the following equation:

$$\left(\frac{\partial (E^2)}{\partial \eta_1} \right)_{\alpha_1} = 0 \qquad (4\text{-}5)$$

Solving Eqn. 4-5, η_1 was calculated to be $5.62\,MPa$ for $\alpha_1 = 0.74$. The value of α_1 was obtained from Eqn. 4-4, which depends on the linear part of the force-stretch curve and is independent of μ_1; thus the change of η_1 does not affect the value of α_1. Finally, η_1 and α_1 were determined to be $5.62\,MPa$ and 0.74 respectively. Plotting the one-term Ogden's equation with $\eta_1 = 5.62 MPa$ and $\alpha_1 = 0.74$ in Fig. 4-3, a good agreement was found with experimental data for stretch ratios up to 1.8.

Having obtained a good fit to the experimental data up to stretch of about 1.8 with a single-term equation, the second term needs to be introduced in order to achieve a good fit to the full range of the data. By employing a single –term equation, the curve fits the data well up to stretch ratio of 1.8, it is only necessary to consider the stretch ratios greater than 1.8.

For α_2 sufficiently greater than zero and $\lambda > 1.8$, the dominant term in $\eta_2 \left(\lambda^{\alpha_2 - 1} - \lambda^{-\alpha_2/2 - 1} \right)$ is $\eta_2 \lambda^{\alpha_2 - 1}$. Neglecting the contribution of $\eta_2 \lambda^{-\alpha_2/2 - 1}$, and moving the

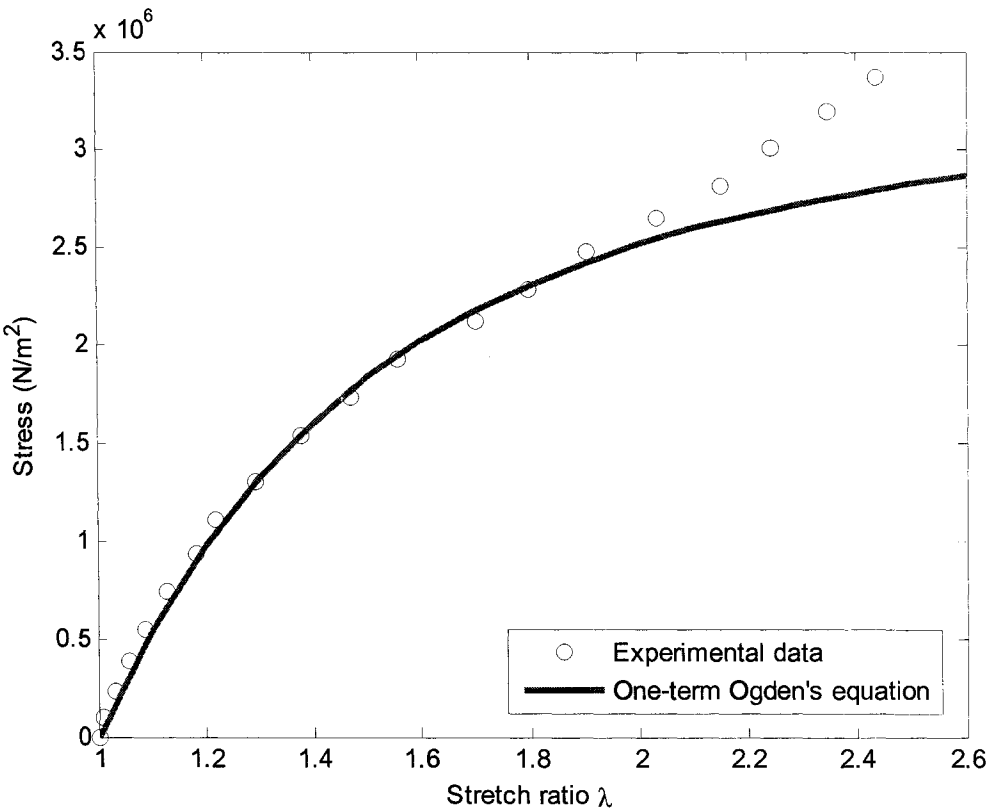

Fig. 4-3 Single term Ogden's equation prediction with $\eta_1 = 5.62MPa$ and $\alpha = 0.74$, compared with silicone stretch-elongation data

first term on the right hand side of the Eqn. 4-1 to the left hand side, the equation becomes

$$\sigma_n - \eta_1\left(\lambda^{\alpha_1-1} - \lambda^{-\alpha_1/2-1}\right) = \eta_2\left(\lambda^{\alpha_2-1} - \lambda^{-\alpha_2/2-1}\right) \approx \eta_2\lambda^{\alpha_2-1} \tag{4-6}$$

Taking the natural logarithm on both side of Eqn. 4-6 yields

$$\ln\left[\sigma_n - \eta_1\left(\lambda^{\alpha_1-1} - \lambda^{-\alpha_1/2-1}\right)\right] \approx \ln\eta_2 + (\alpha_2 - 1)\ln\lambda$$

For stretches above 1.8, η_2 and α_2 were obtained by plotting

$\ln\left[\sigma_n - \eta_1\left(\lambda^{\alpha_1-1} - \lambda^{-\alpha_1/2-1}\right)\right]$ versus $\ln\lambda$ as shown in Fig.4-4. The slope is

approximately $\alpha_2 - 1$, and the intercept is $\ln \eta_2$.

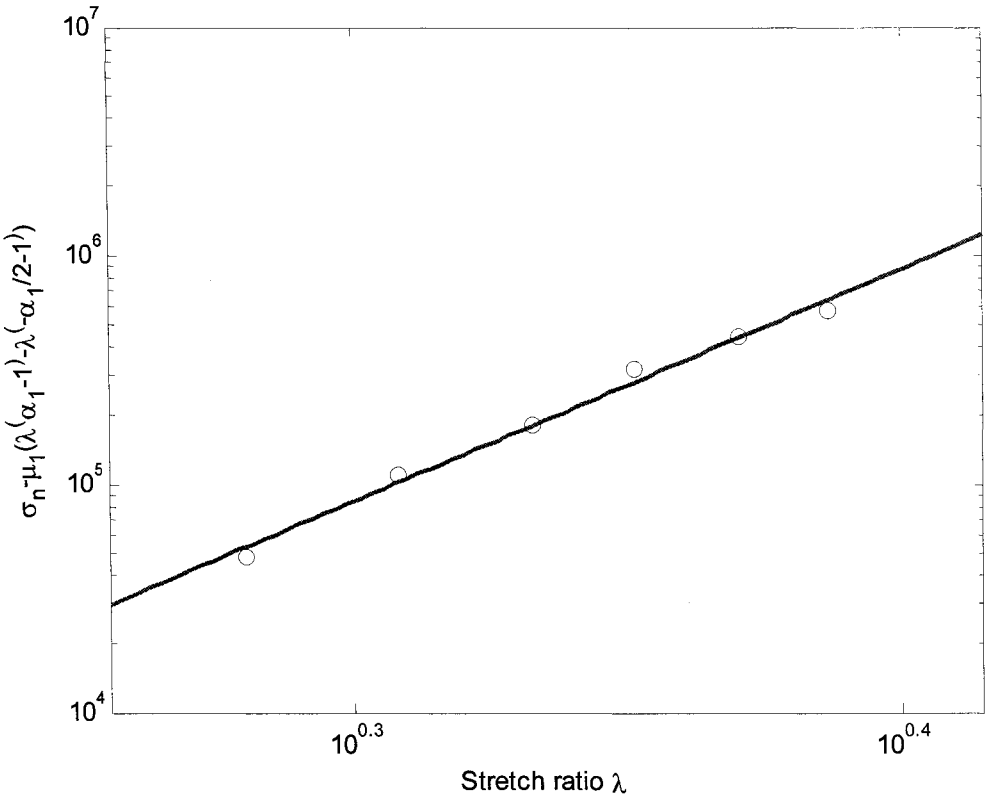

Fig. 4-4 $\ln[\sigma_n - \eta_1(\lambda^{\alpha_1-1} - \lambda^{-\alpha_1/2-1})]$ versus $\ln \lambda$ for silicone rubber

Examining Fig. 4-4, the values of η_2 and α_2 were found to be $7.85 \times 10^{-5} MPa$ and 11.12 respectively.

The four coefficients of the two-term Ogden's equation for silicone rubber were determined to be:

$$\eta_1 = 5.62MPa \qquad \eta_2 = 7.85 \times 10^{-5} MPa$$

$$\alpha_1 = 0.74 \qquad \alpha_2 = 11.12$$

The two-term Ogden's equation compared with silicone rubber stress-stretch data is given in Fig. 4-5. The fit is now very good up to a stretch ratio of 2.4.

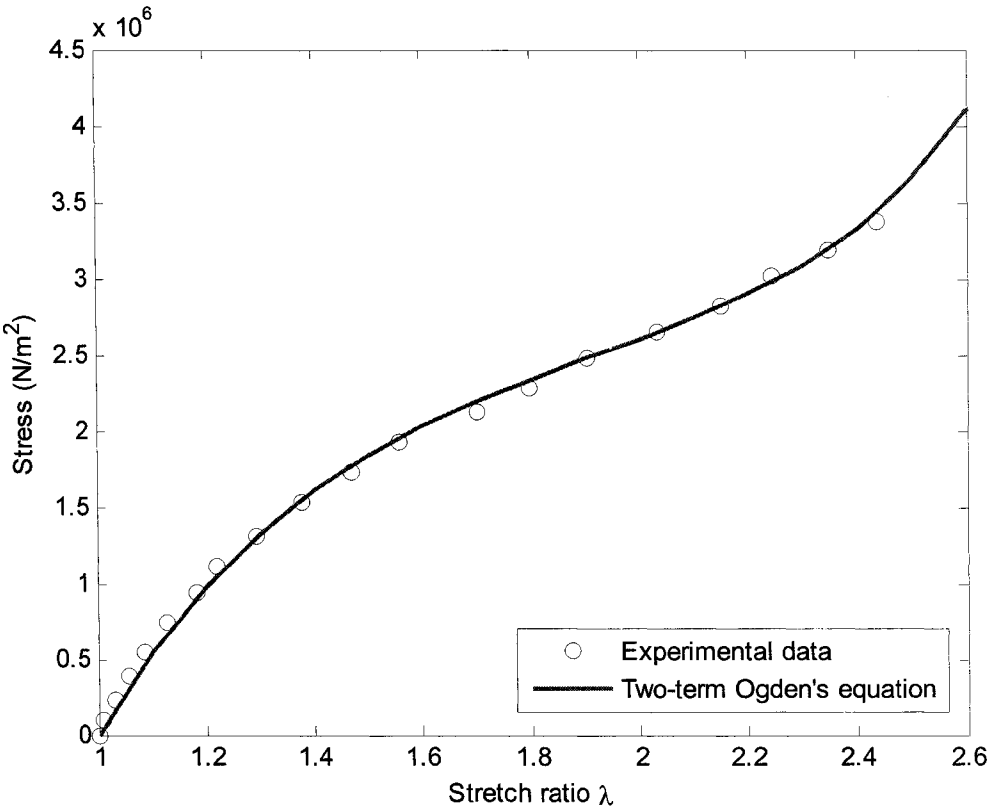

Fig. 4-5 Two-term Ogden's equation compared with silicone rubber stress-stretch data.

Following the same procedure, the four coefficients of the two-term Ogden's equation for EPDM are:

$$\eta_1 = 2.01MPa \qquad \eta_2 = 2.00\times10^{-4}\,MPa$$

$$\alpha_1 = 0.73 \qquad \alpha_2 = 11.57$$

A two-term Ogden's equation with the above coefficients was plotted and compared with EPDM stress-stretch data. The Ogden's model is in good agreement with experimental data as shown in Fig. 4-6.

In using Ogden's equation for describing the stress-stretch relationship, a question arises regarding the physical interpretation of the parameter, η_1, α_1, μ_2 and α_2.

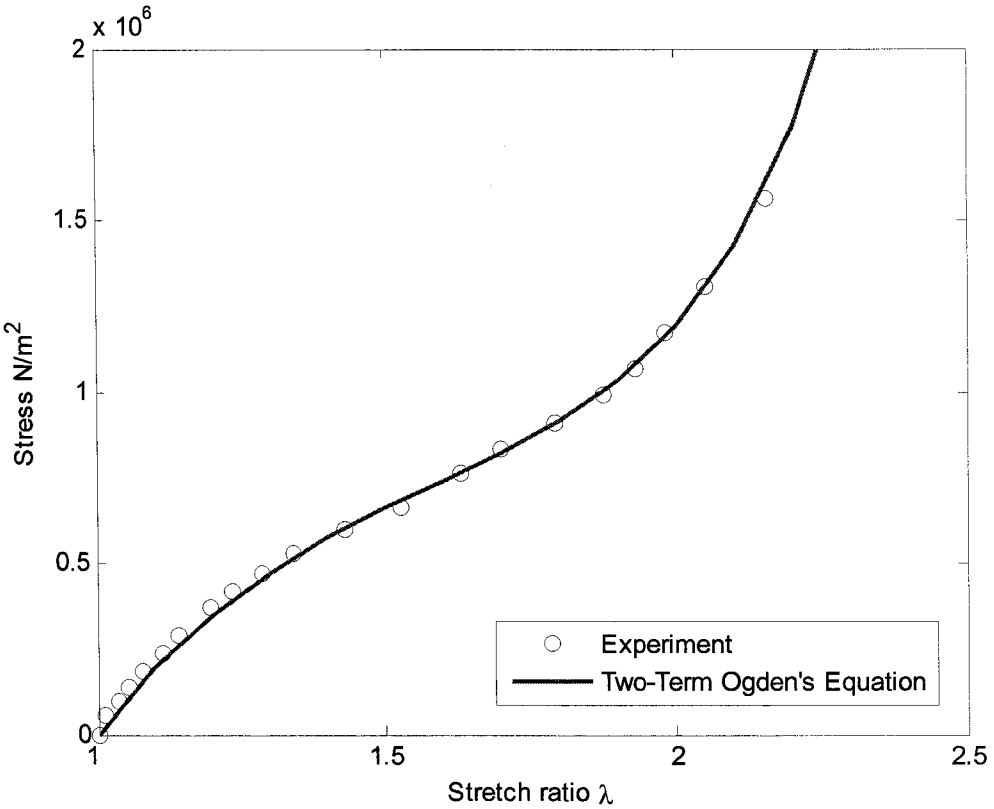

Fig. 4-6 Two-term Ogden's equation compared with EPDM stress-stretch data.

In the low stretch range, the rubber stress-stretch relationship is nearly linear, and a single-term Ogden's equation is capable of describing such a relationship. Thus, a single-term Ogden's equation was used for simplifying the derivation to describe the stress-stretch relationship according to Eqn. 2-10.

$$\sigma_i = \eta_1 \lambda_i^{\alpha_1} - P \tag{4-7}$$

Expanding Eqn. 4-7 in Taylor's series about λ equal to 1 yields

$$\sigma_i = \sigma_i\big|_{\lambda=1} + \sigma_i'\big|_{\lambda=1}(\lambda-1) + \frac{\sigma_i''\big|_{\lambda=1}}{2!}(\lambda-1)^2 + \cdots \tag{4-8}$$

$$= \eta_1 - P + \eta_1\alpha_1(\lambda-1) + \frac{1}{2}\eta_1\alpha_1(\alpha_1-1)(\lambda-1)^2 + \cdots$$

Since the strain, $\varepsilon = \lambda - 1$, is in the small deformation range, neglecting higher order terms, Eqn.4-8 becomes

$$\sigma_i = \eta_1 - P + \eta_1 \alpha_1 \varepsilon_i \tag{4-9}$$

For a uni-directional stretch, $\sigma_1 = \sigma$, $\sigma_2 = \sigma_3 = 0$ and $\varepsilon_1 = \varepsilon$, $\varepsilon_2 = \varepsilon_3 = -\frac{1}{2}\varepsilon$ for small deformation where it is assumed that Poisson's ratio is 0.5. Substituting σ_1, σ_2, ε_1 and ε_2 into Eqn. 4-9 yields

$$\sigma = \eta_1 - P + \eta_1 \alpha_1 \varepsilon$$

and

$$0 = \eta_1 - P + \eta_1 \alpha_1 (-\frac{1}{2}\varepsilon)$$

Eliminating P leads to

$$\sigma = \frac{3}{2}\eta_1 \alpha_1 \varepsilon \tag{4-10}$$

For small stretch ratios, the stress-strain relationship is approximately linearly elastic, and can be explained by Hook's law,

$$\sigma = E\varepsilon \tag{4-11}$$

where E is Young's modulus. Equating Eqn. 4-10 and Eqn. 4-9 shows the relationship between Young's modulus and Ogden's parameters

$$E = \frac{3}{2}\eta_1 \alpha_1 \tag{4-12}$$

The shear modulus, G is related to E and Poisson's ratio, v

$$G = \frac{E}{2(1+v)} \tag{4-13}$$

For an ideal rubber, with a Poisson's ratio of 0.5, Eqn. 4-13 becomes

$$G = \frac{E}{3}$$

Thus, the product of the Ogden's parameters $\mu_1\alpha_1$ is related to the shear modulus of rubber

$$2G = \eta_1\alpha_1 \tag{4-14}$$

Since α_1 was shown to be close to 0.75 for both silicone rubber and EPDM, η_1 is approximately three times the shear modulus of rubber. Although rubbers are not linearly elastic, the relationship in Eqn. 4-12 does provide some basis that higher values of $\eta_1\alpha_1$ leads to higher rubber shear modulus.

4.3 Validation of Desorption Technique for Rubber in Stress-Free State

Most of the literature data of gas sorption in rubber are for the stress-free state. In order to check the reliability of the current test methodology, the CO_2 solubility in rubber in the stress-free state must be measured for comparison. Preliminary results are presented for the solubility of CO_2 in silicone rubber in Fig. 4-7 at a temperature of 20°C. The data obtained for CO_2 in silicone rubber were compared with data from [3, 7]. Unfortunately, these data are not exactly comparable because they were taken at 35°C, while the tests were conducted at 20°C; however, they do provide some basis for comparing the desorption technique with the barometric technique used by Pope et al. and Fleming and Koros.

For pressures below 1.4 *MPa*, the data obtained in this study lie between the two sets of data obtained from the literature, while for pressures above 1.4 *MPa*, the current data is above the two literature values. It is believed that the data from Pope et al. [7] are

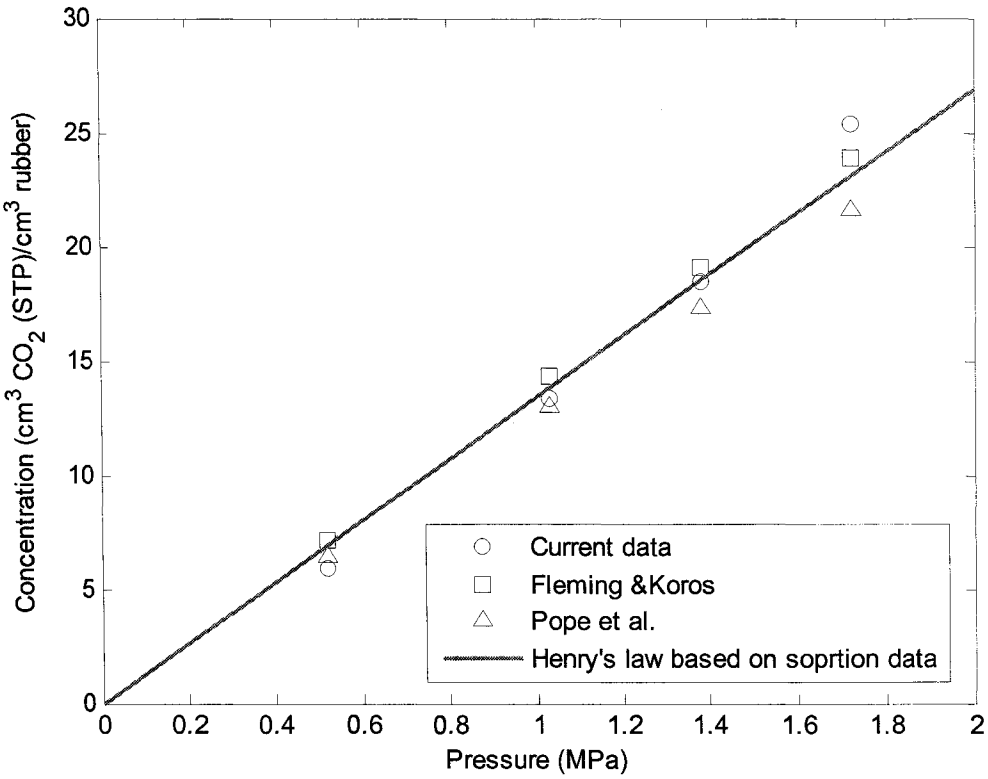

Fig. 4-7 Sorption isotherm of carbon dioxide in silicone rubber at 20°C and comparison with literature data

more accurate than those of the initial tests done by Fleming and Koros [3]. The present measurements yield solubilities that are larger than those of Pope, et al. [7] and larger than Fleming and Koros at $1.72\,MPa$. This is consistent with the effect of temperature on solubility of gas in polymers; equilibrium solubility generally decreases with an increase in temperature. Although the data at $0.52\,MPa$ is lower than Pope's data, the weight loss associated with these low solubilities are small and have a large error due to the resolution of the analytical balance. Thus, the data of the desorption technique are in the right range for solubility of CO_2 in silicone rubber, and the results show that the method used in this study is valid.

Examining Fig.4-7, a linear relation between gas pressure and gas concentration

was found for the concentrations up to about $18.4\,cm^3\ CO_2\ (STP)/cm^3 rubber$, and can be explained by the Henry's law. The Henry's law constant for that concentration range is 13.06 $cm^3\ (STP)/(cm^3\ rubber\ MPa)$, which is in good agreement with the value of 13.71 $cm^3\ (STP)/(cm^3\ rubber\ MPa)$ given by Fleming and Koros. At higher pressures and gas concentrations, the data deviates slightly from Henry's law, which could be explained by a Flory-Huggins theory as shown in Eqn. 4-15.

$$\ln\frac{P}{P_0} = \ln(1-\phi_2) + \phi_2 + \chi\phi_2^{\,2} \tag{4-15}$$

where P is the gas pressure, P_0 is the vapor pressure at 20°C, χ is the Flory-Huggins parameter, and ϕ_2 is the polymer volume fraction and given by

$$\phi_2 = 1-\phi_1 = 1-\frac{CV_g/22410}{1+CV_g/22410} = \frac{1}{1+CV_g/22410} \tag{4-16}$$

where ϕ_1 is the volume fraction of CO_2, and V_g is the partial molar volume of CO_2 (cm^3/mol),

In order to find χ in the Flory-Huggins theory, the partial molar volume and the vapor pressure of CO_2 must be determined. The partial molar volume of CO_2 can be obtained from the dilation measurement. It is assumed that the partial molar volume of stress-free rubber is the same as deformed rubber, and this will be discussed later. For a rubber band, it is hard to measure the width in stress-free state because of curling effect; thus, only the stretched rubber band dilation was measured. The dilation measurements are presented in Table 4-2 and Table 4-3 for silicone rubber and EPDM respectively.

According to other researchers, [3], the dilation ratios of thickness and width are exactly the same, which implies that rubber undergoes isotropic swelling. Thus, the

Table. 4-2 Width dilation measurement of silicone rubber at 20°C.

Pressure (*MPa*)	stretch ratio=1.52	stretch ratio=1.94
0	1.0000	1.0000
0.52	1.0069	1.0075
1.03	1.0138	1.0143
1.38	1.0180	1.0183
1.72	1.0258	1.0260

Table. 4-3 Width dilation measurement of EPDM at 20°C.

Pressure (*MPa*)	stretch ratio=1.47	stretch ratio=1.88
0	1.0000	1.0000
0.52	1.0035	1.0036
1.03	1.0071	1.0070
1.38	1.0090	1.0094
1.72	1.0120	1.0120

thickness and width dilation ratios were treated as the same without further measurement.

For the stretched rubber sample, the length in the X-direction is fixed as described in Chapter 2, and the volume dilation ratio was taken as the square of the width dilation ratio. Figure 4-8 shows silicone rubber volume dilation percentage obtained from the volume dilation ratios for the stretch ratios of 1.52 and 1.94.

With the sorption and dilation data, it is straightforward to determine the partial specific volumes of the silicone rubber and CO_2, and then obtain the partial molar volume. The partial specific volume is defined as the increase of volume upon addition of a unit mass of a gas (cm^3 / g_{gas}), while the partial molar volume is defined as the increase of volume upon addition of a mole of molecules of a gas (cm^3 / mol_{gas}). Plotting the specific volume of the gas-laden rubber against the mass fraction of CO_2 (defined as the mass of

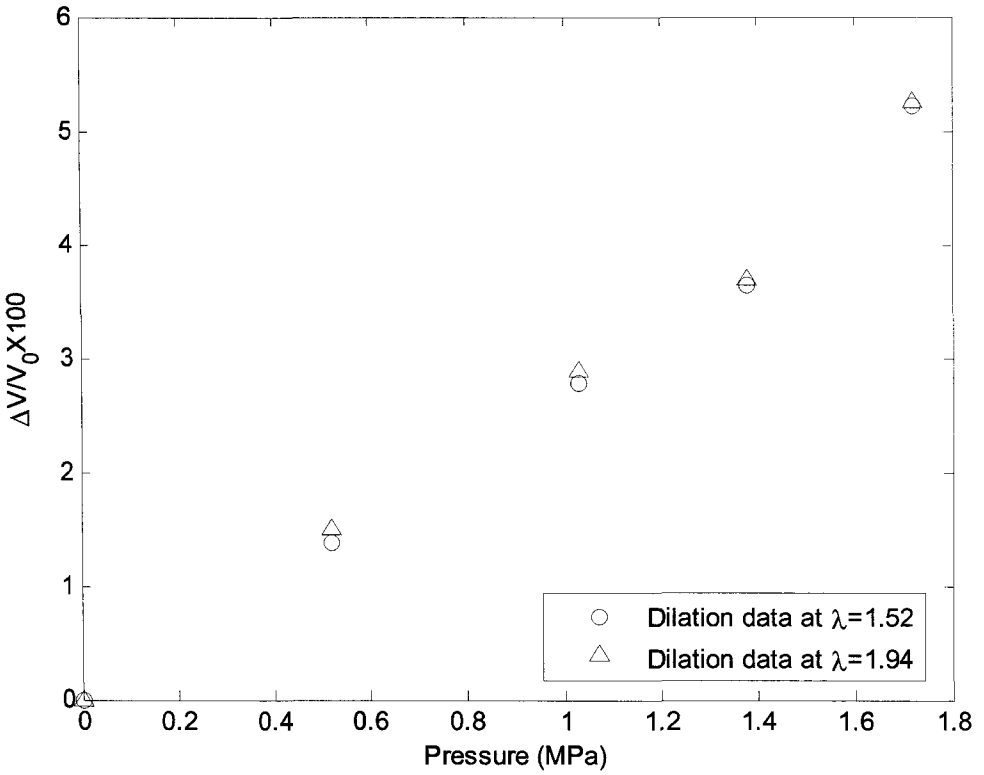

Fig. 4-8 Volume dilation percentages of silicone rubber saturated with CO_2 under stretch ratios of 1.52 and 1.94

CO_2 percentage in gas-laden rubber) as shown in Fig.4-9, the gas partial specific volume of the gas-laden polymer can be determined from the slope of the curve, where the specific volume is defined as volume per unit mass of the gas-laden rubber. Figure. 4-9 shows that the specific volume of gas-laden silicone rubber versus CO_2 mass fraction is approximately a straight line in the range of the CO_2 mass fraction studied; thus the partial specific volume of CO_2 in this range can be treated as a constant value, and determined from the intercept of the straight line at w_{CO_2} equal to 1, where w_{CO_2} is the CO_2 mass fraction.

The calculated partial specific volumes of CO_2 in silicone rubber and EPDM at

20°C are given in Table 4-4 and Table 4-5 respectively. The data shows that the partial specific volume for stretch of 1.52 and 1.94 is approximately the same. Thus, the assumption made before that the partial specific volume of CO_2 in rubber in a stress-free state is the same as that for stressed rubber is valid. Furthermore, the conclusion can be made that the partial specific volume is independent of the stress-stretch state in the range of the current study. An average value of CO_2 partial specific volume is used hereafter.

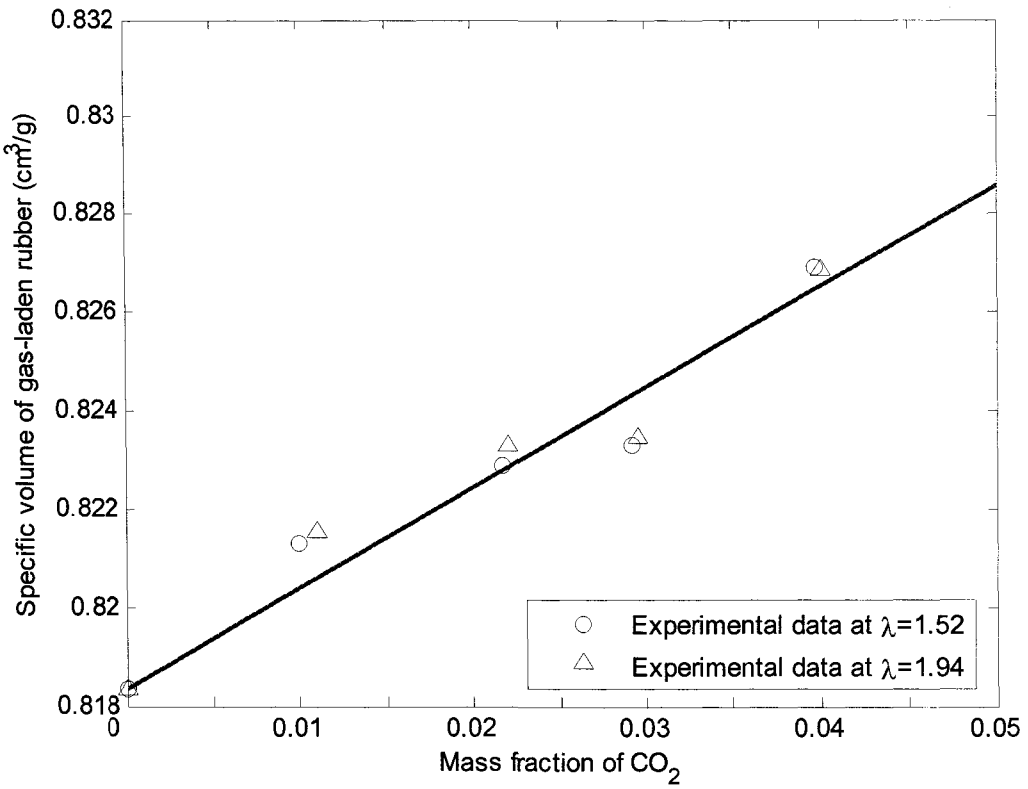

Fig. 4-9 Specific volume of the gas-laden silicone rubber sample vs. CO_2 mass fraction at 20°C

Table. 4-4 CO_2 partial specific volume in silicone rubber under stretch

Stretch ratio	Partial specific volume (cm^3/g)
1.52	1.023
1.94	1.025
Average value	1.024

Table. 4-5 CO_2 partial specific volume in EPDM under stretch

Stretch ratio	Partial specific volume (cm^3/g)
1.47	1.043
1.88	1.041
Average value	1.042

The partial molar volume of CO_2 in silicone rubber, V_g is determined to be 45.06 cm^3 / mol by converting the partial specific volume given in Table 4-4 and 4-5 to a molar volume (i.e. multiplying by molecular weight of CO_2). For EPDM, the partial molar volume is 45.85 cm^3 / mol. Fleming and Koros [3] have measured the partial molar volume of CO_2 in silicone rubber at 35°C, and their value was 46.2 cm^3 / mol. Hirose et al. [34] have measured the partial molar volume of CO_2 in low-density polyethylene over a temperature range of 25 to 55°C and observed no strong temperature dependence for the partial molar volume on the sorbed CO_2. The average molar volume that Hirose et al. measured for the polyethylene/CO_2 system in the temperature range 25-55°C was 44.5 cm^3 / mol. Both Fleming & Koros and Hirose's measurement are in good agreement with the current partial molar volume of CO_2 in silicone rubber and EPDM. Rubbery polymers are equilibrium solids, and the interactions of gases with rubbery polymers and low molecular weight liquids have been shown to be very similar [30]. The infinite dilution partial molar volumes for CO_2 in various low molecular weight liquids measured by Horuiti [31] and Reid et al. [25] were shown to be insensitive to the type of medium and decrease only slightly as interactions between the medium and CO_2 increase. The average value of the partial molar volume for the CO_2 at infinite dilutions at 25°C is approximately 46 cm^3 / mol is also close to the current data. As for the carbon dioxide

partial molar volume in EPDM, no literature value was found. According to the works of Horuiti and Reid et al., the partial molar volume in silicone rubber and in EPDM should be close to each other, which is in good agreement with this study.

Another parameter required for Eqn. 4-15 is the CO_2 vapor pressure at 20°C. The Frost-Kalkwarf-Thodos vapor pressure equation [25] was employed to evaluate the CO_2 vapor pressure:

$$\ln P_{vpr} = B\left(\frac{1}{T_r} - 1\right) + C\ln T_r + \frac{27}{64}\left(\frac{P_{vpr}}{T_r^{\,2}} - 1\right) \tag{4-17}$$

where $P_{vpr} = \frac{P_{vp}}{P_c}$, P_{vp} is the vapor pressure at 20°C, P_c is critical pressure, $T_r = \frac{T}{T_c}$, T_c is the critical temperature. The coefficients B and C are defined as:

$$B = \frac{\ln P_c + 2.67\ln T_{br} + \frac{27}{64}\left(\frac{1}{P_c T_{br}^{\,2}} - 1\right)}{1 - \frac{1}{T_{br}} - 0.7816\ln T_{br}} \tag{4-18}$$

where $T_{br} = \frac{T_b}{T_r}$, T_b is the boiling temperature at ambient pressure of the tests, which is atmospheric pressure. The constant C is defined as,

$$C = 0.7816B + 2.67 \tag{4-19}$$

For CO_2, $P_c = 7.38MPa$, $T_c = 304.2K$, $T_b = 194.7K$ at atmospheric pressure.

Substituting Eqn. 4-18 and 4-19 into Eqn. 4-17, the vapor pressure was calculated to be 5.51 MPa at 20°C.

Instead of measuring it, the Flory-Huggins parameter was obtained by solving the Flory-Huggins equation with gas sorption measurement for zero stretch. For each measured sorption value, a value of χ was obtained and given in Table. 4-6. And an

average value, 1.04, was taken as the Flory-Huggins parameter for silicone rubber/CO_2 sorption isotherm; 1.71 was the calculated Flory-Huggins interaction parameter for the EPDM/CO_2 system at 20°C.

Table. 4-6 Calculated values of Flory-Huggins parameter, χ

Pressure (*MPa*)	0.52	1.03	1.38	1.72	Average value
Silicone rubber/CO_2	1.03	1.05	1.09	0.99	1.04
EPDM/CO_2	1.69	1.76	1.72	1.69	1.71

The Flory-Huggins predictions for equilibrium gas solubilities using the average value of χ and measurements are shown in Figs. 4-10 and 4-11 for silicone rubber and EPDM, respectively. Henry's law constant was determined by using the measured gas concentration at 0.52, 1.04, and 1.38 *MPa* was also plotted for comparison. Figure 4-10 and 4-11 show that at low gas concentrations, Henry's law predictions are in good agreement with experiment, while above that range, evident deviation from Henry's law was found, and a Flory-Huggins theory gives good agreement for the full pressure range. The work done by Fleming and Koros [3] has proven for silicone rubber/CO_2 system, the Flory-Huggins theory gave good predictions for pressures up to 5.6 *MPa* .

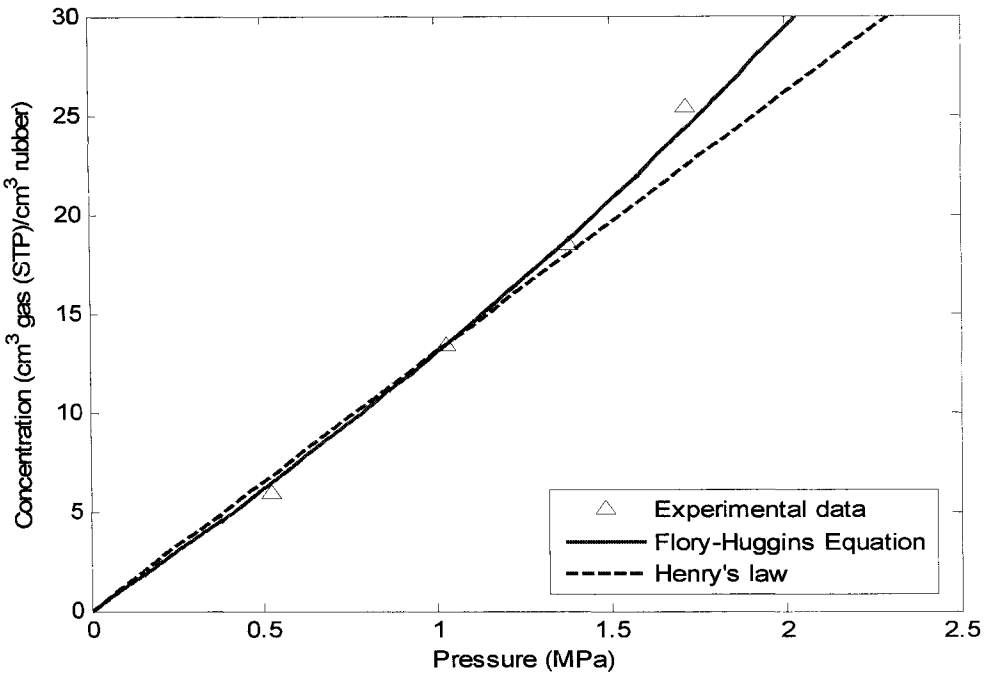

Fig. 4-10 Flory-Huggins equation and Henry's law compared with experimental data in silicone rubber/CO_2 for stress free-state at 20°C.

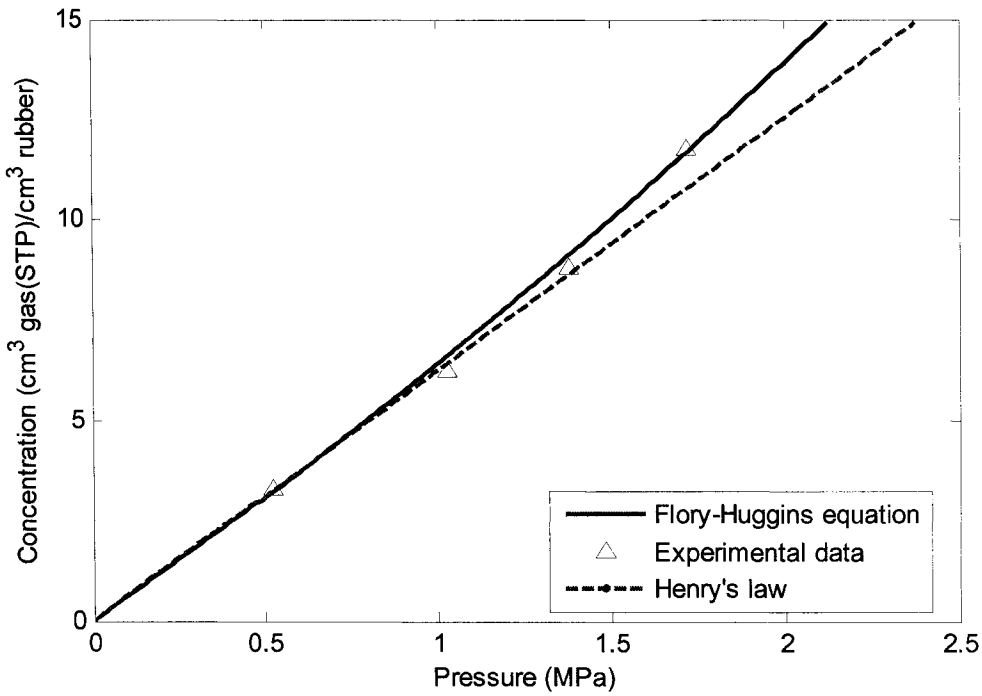

Fig. 4-11 Flory-Huggins equation and Henry's law comparison with experimental data in EPDM/CO_2 for stress free-state at 20°C.

4.4 CO_2 Sorption in Rubber under Uni-axial Stretch

The sorption data of CO_2 in silicone rubber and EPDM under different stretch ratios at 20°C are summarized in Table 4-7 and Table 4-8, respectively. For each pressure level and stretch ratio, at least 3 tests were conducted to check the repeatability and estimate the standard deviations for the measurement.

Table. 4-7 Concentration of CO_2 in silicone rubber [cm^3 CO_2 (STP)/cm^3rubber] at 20°C .

	0.52MPa	1.03MPa	1.38MPa	1.72MPa
λ=1				25.44
	5.91	13.44	18.35	25.44
	5.79	13.44	18.60	25.32
	5.97	13.19	18.35	25.51
Average	5.89	13.35	18.44	25.43
Standard Deviation	0.10	0.14	0.14	0.08
λ=1.5	6.35	13.87	18.72	25.69
	6.29	13.75	18.72	25.82
	6.03	13.87	18.85	25.63
Average	6.22	13.83	18.77	25.63
Standard Deviation	0.16	0.072	0.072	0.10
λ=1.9	6.91			25.88
	6.97	13.94	18.97	26.00
	6.91	14.06	19.16	25.88
	6.84	14.25	18.91	25.94
Average	6.91	14.08	19.02	25.93
Standard Deviation	0.05	0.16	0.13	0.06

Table. 4-8 Concentration of CO_2 in EPDM [cm^3 CO_2 (STP)/cm^3 rubber] at 20°C.

	0.52MPa	1.03MPa	1.38MPa	1.72MPa
λ=1		6.31		
	3.29	6.26	8.78	11.63
	3.35	6.26	8.89	11.85
	3.24	6.15	8.73	11.80
Average	3.29	6.24	8.80	11.74
Standard Deviation	0.05	0.07	0.08	0.10
λ=1.5	3.40	6.70	8.84	11.85
	3.35	6.81	8.95	11.85
	3.35	6.81	8.89	11.63
Average	3.47	6.76	8.89	11.78
Standard Deviation	0.03	0.06	0.05	0.13
λ=1.9	3.40	7.08	9.27	
	3.51	6.97	9.33	11.80
	3.56	6.91	9.16	11.80
	3.40	6.97	9.16	11.74
Average	3.47	6.98	9.23	11.80
Standard Deviation	0.08	0.07	0.08	0.03

In order to show the effect of stretch on Henry's law constant, only the data below 1.38 *MPa* were plotted in Fig. 4-12 and Fig. 4-13 for silicone rubber/CO_2 and EPDM/CO_2 respectively, because at higher pressure or concentration, a slight deviation was found from the Henry's law prediction, which will be discussed later. The figures show that Henry's law predictions are still valid in the low concentration range for CO_2 sorption in silicone rubber and EPDM under unidirectional stretch, but the Henry's law constants are affected by stretch. Higher stretch ratios result in higher Henry's law constant and this is shown in Table 4-9. Although the difference of the Henry's law constants is rather small, the effect of the stretch on CO_2 solubility in rubber is identifiable.

Table. 4-9 Henry's law constant of CO_2 in silicone rubber and EPDM under different stretch ratios at 20°C [cm^3 gas (STP)/ (cm^3 polymer *MPa*)]

	$\lambda = 1$	$\lambda = 1.5$	$\lambda = 1.9$
Silicone rubber	13.06	13.41	13.70
EPDM	6.27	6.48	6.72

The thermodynamic model of gas sorption in rubber under uni-axial stretch developed in Section 2 needs to be introduced to describe the full CO_2 sorption isotherm:

$$kT \ln \frac{P}{P_0} = kT\left[\ln(1-\phi_2) + \phi_2 + \chi\phi_2^{\,2}\right]$$

$$+ \frac{V_0}{2N_0}\sum_{r=1}^{n}\eta_r\left[\left(\lambda\phi_2^{1/2}\right)^{-\alpha_r/2} - \left(\lambda\phi_2^{1/2}\right)^{\alpha_r} - \left(\phi_2^{1/2}\right)^{-\alpha_r/2} + \left(\phi_2^{1/2}\right)^{\alpha_r}\right] + PV_0\frac{\phi_2}{N_0} \qquad (4\text{-}20)$$

where ϕ_2, N_0 and P_0 are given by

$$\phi_2 = \frac{1}{1 + CV_g/22410}$$

$$N_0 = \frac{C/22410}{1-\phi_2} \times 6.022 \times 10^{23}$$

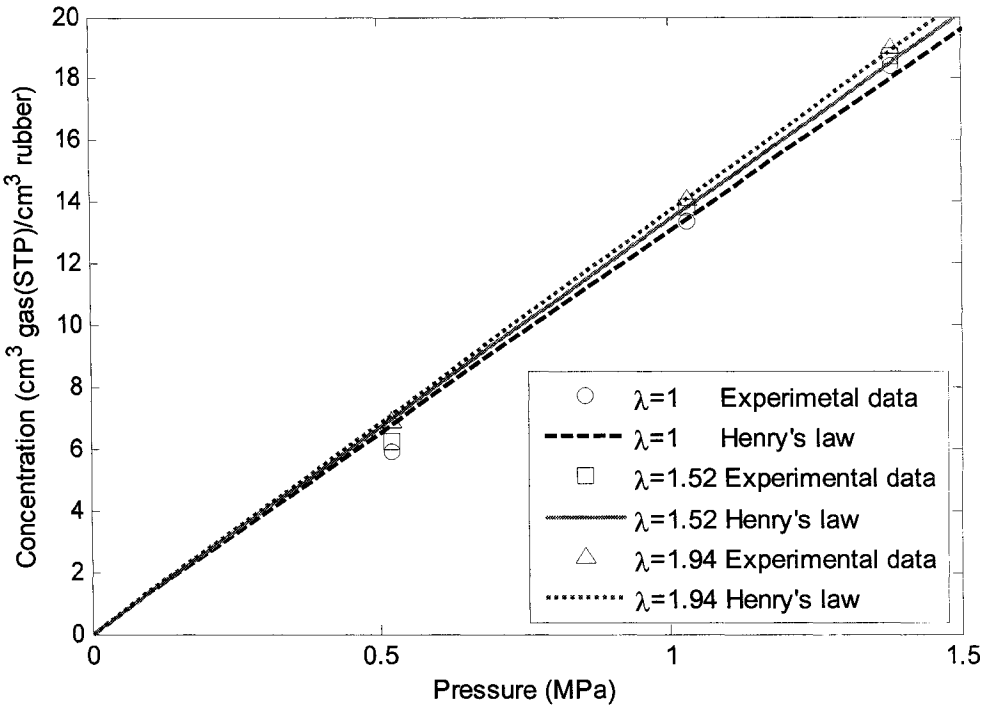

Fig. 4-12 CO_2 sorption isotherm in silicone rubber under different stretch ratios at 20°C. Lines through the data are linear least square fit.

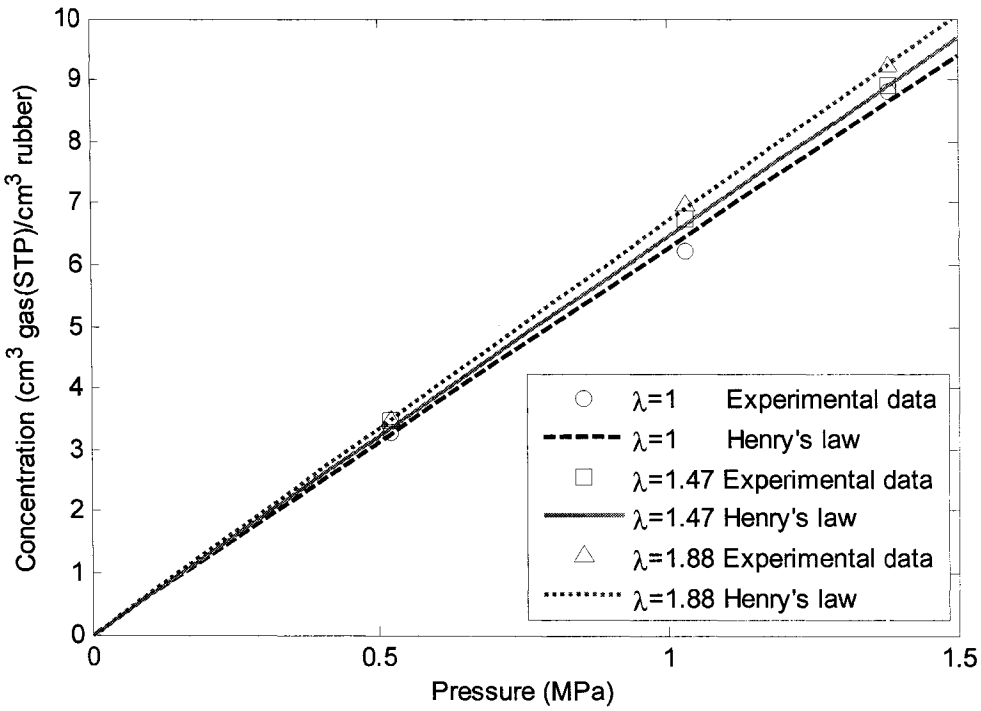

Fig. 4-13 CO_2 sorption isotherm in EPDM under different stretch ratios at 20°C. Lines through the data are linear least square fit

$P_0 = 5.51 MPa$

The partial molar volumes of CO_2 in silicone rubber and EPDM are $45.06\, cm^3 / mol$ and $45.85\ cm^3 / mol$ respectively. The four coefficients of Ogden's equation of silicone rubber stress-strain were determined to be:

$$\eta_1 = 5.62 MPa \qquad \eta_2 = 7.85 \times 10^{-5}\ MPa$$

$$\alpha_1 = 0.74 \qquad \alpha_2 = 11.12$$

while for EPDM, the coefficients are

$$\eta_1 = 2.01 MPa \qquad \eta_2 = 2.00 \times 10^{-4} MPa$$

$$\alpha_1 = 0.73 \qquad \alpha_2 = 11.57$$

Since the Flory-Huggins parameter, χ is defined as:

$$\chi = \frac{(z-2)}{kT} \Delta u_{12}$$

it is a function of temperature and solute –solvent segment interaction energy, and does not depend on stretch ratio. Thus, the Flory-Huggins parameter obtained from the zero-stretched rubber/CO_2 should be able to be applied to Eqn. 4-19 to predict gas sorption in rubber under uni-axial stretch. In order to verify this, the Flory-Huggins parameter, χ was calculated for each stretch ratio, and is presented in Table. 4-10. Examining Table 4-10, it was found that for the current stretch range, the stretch has no significant effect on the Flory-Huggins parameter and the Flory-Huggins parameter determined from the zero stretch rubber was used hereafter.

The test results are compared with the theory of gas sorption in rubber with uni-directional stretch in Fig. 4-14 and Fig. 4-15 for silicone rubber/CO_2 and EPDM/CO_2 respectively. The model prediction using Eqn. 4-20 show that for a stretch of 1.9 and a

Table. 4-10 The calculated Flory-Huggins Parameters for silicone rubber/CO_2 and EPDM/CO_2

	$\lambda = 1$	$\lambda = 1.5$	$\lambda = 1.9$	Average
Silicone rubber/CO_2	1.04	1.05	1.04	1.04
EPDM/CO_2	1.71	1.69	1.67	1.69

CO_2 pressure of 1.72 *MPa* , the increase in CO_2 gas solubility in silicone rubber is approximately 3.5%; the measured increase is 2%. The measured and predicted changes are relatively small but the trends in the measured data are predicted by the model.

A comparison of the predicted changes in CO_2 solubility with stretch for silicone rubber and EPDM show that the changes in solubility for silicone rubber should be larger than for EPDM. The product $\eta_1\alpha_1$ (related to the rubber shear modulus) is 4.16 *MPa* for silicone rubber compared with 1.47 *MPa* for EPDM, which indicts that the shear modulus of silicone rubber should be higher than that of EPDM. Rubber with larger shear modulus should have a greater increase in gas solubility due to stretch than rubber with smaller shear modulus. The increase of CO_2 solubility in silicone rubber and EPDM at the maximum stretch is 3.5% and 1% compared with zero stretch at 1.72 *MPa* . This is shown in the experimental data where the change in CO_2 solubility at the maximum stretch and highest pressure for silicone rubber is 2% compared with 0.5% for EPDM.

Error in the measurements may contribute to the deviations between theoretical predictions and experimental data, since the stretch effect on gas solubility is fairly small. The variation of the room temperature may be another reason since no active temperature control facilities were employed.

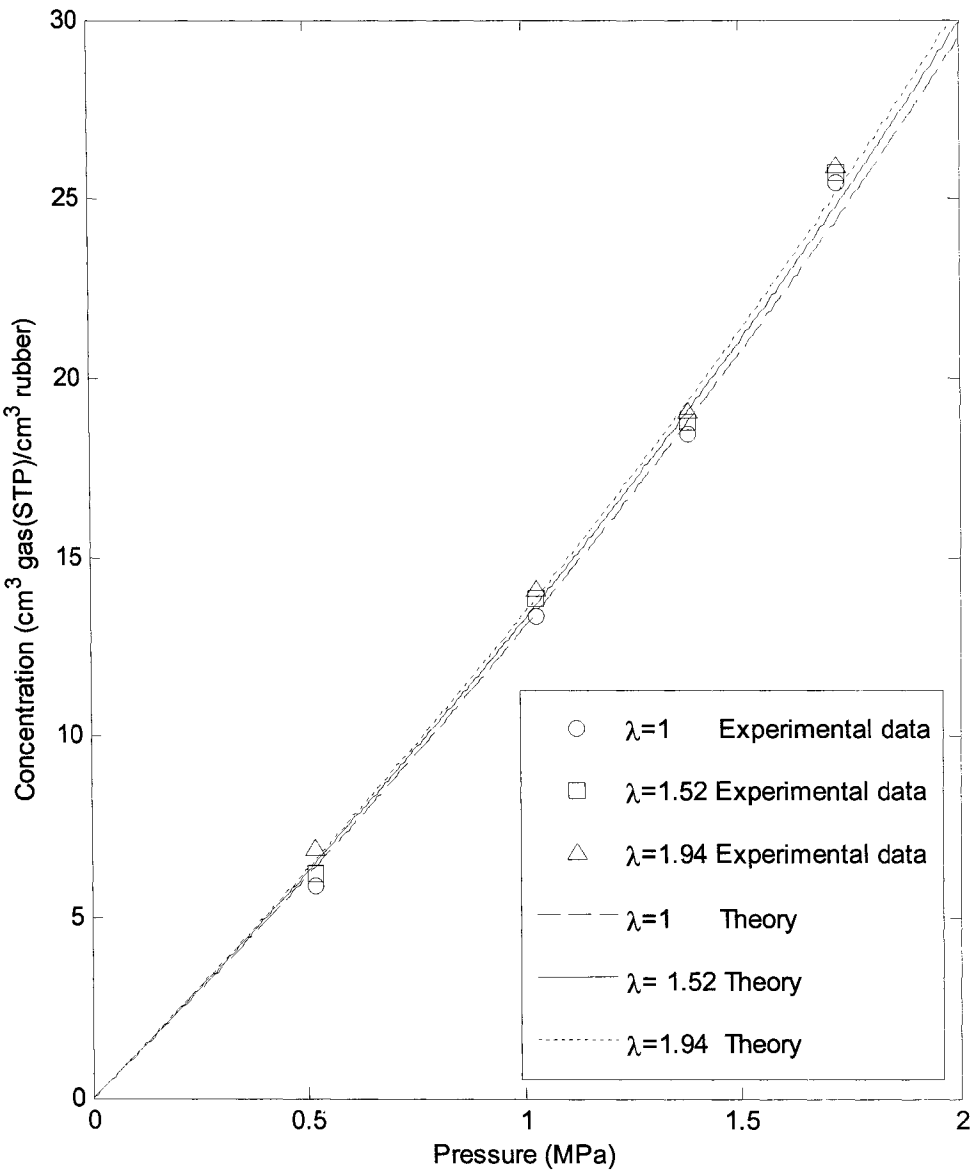

Fig. 4-14 Silicone rubber/CO_2 sorption isotherm with stretch at 20°C

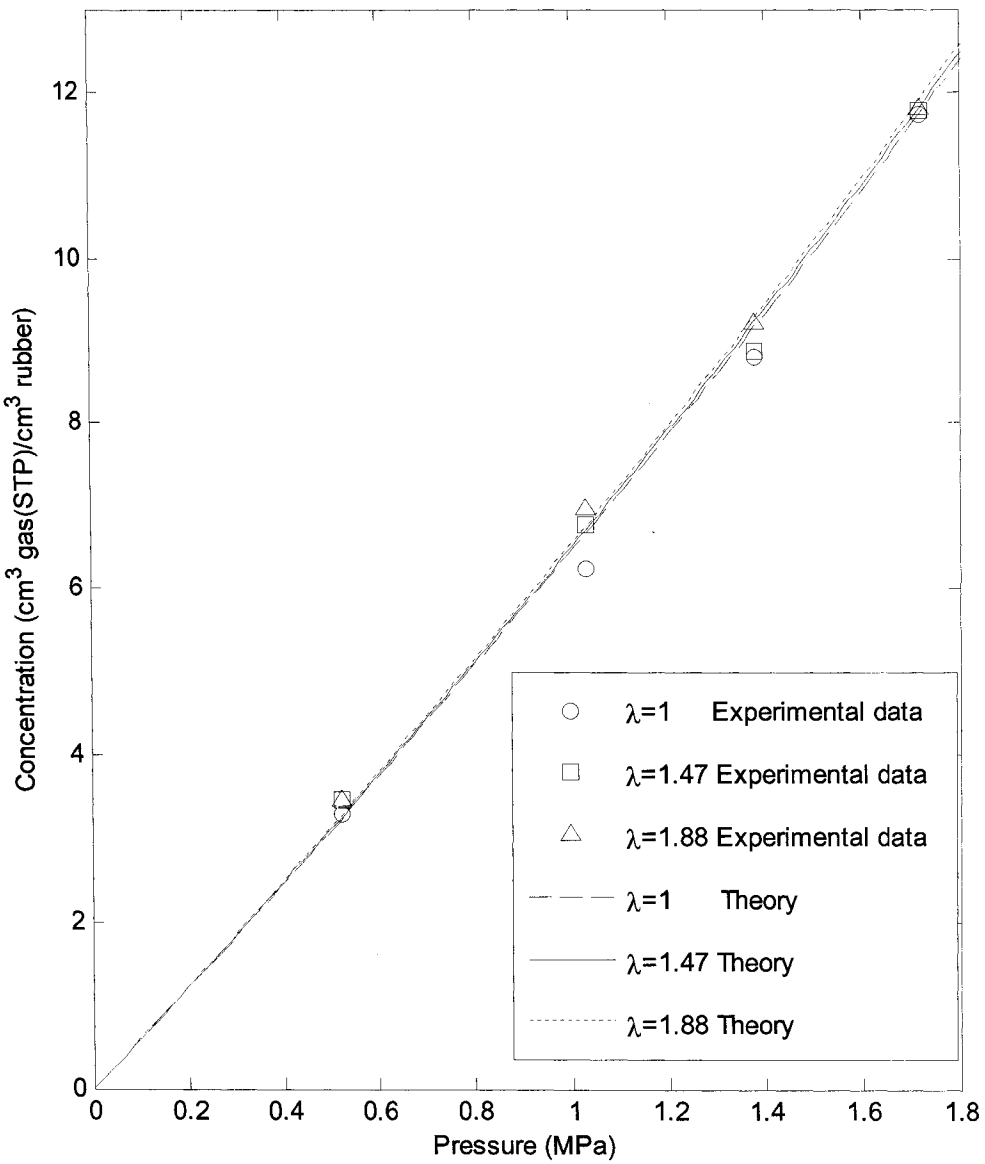

Fig. 4-15 EPDM/CO_2 sorption isotherm with stretch at 20°C

5. Conclusion and Recommendations for Further Research

5.1 Conclusions

The principle conclusions of this work are:

(1) The desorption method is capable of measuring the gas sorption in rubber under stretch. The measured CO_2 solubilities in zero-stretched silicone rubber were in good agreement with literature values.

(2) For zero stretch, the CO_2 sorption isotherm in rubber can be described satisfactorily by Henry's law for pressures up to $1.38\,MPa$. Above that pressure, slight deviations from Henry's law were observed, and a Flory-Huggins model can be used to explain the deviations.

(3) The partial molar volume of CO_2 in stressed silicone rubber is approximately the same as the values reported in silicone rubber in a stress-free state [1], which means that the stretch has no significant effect on partial molar volume.

(4) The stretch has no significant effect on the Flory-Huggins parameter and supports the assumption that the Helmholtz free energies change due to mixing and deformation are independent of each other is valid.

(5) Introducing the Ogden's model for rubber elasticity, a thermodynamic model was developed based on Flory-Huggins theory. The model provided a reasonable agreement with experimental data for the pressure range studied. When a stressed rubber sample was involved, identifiable but insignificant effect of stretch on gas solubility was observed: higher stretch ratio leads to higher solubility and higher Henry's law constant at the same gas pressure. Based on this model, the stretch has more significant effect on gas sorption for rubbers with higher shear modulus.

5.2 Recommendation for Future Study

(1) Future tests should be done on rubbers with higher shear modulus than used in the current study in order to get more significant effect of stretch on gas solubility in rubber.

(2) In this study, only uni-direction extension was considered. Since the Ogden's model is able to describe many kinds of deformations, such as simple tension, equi-biaxial, pure shear, and simple shear; it is straightforward to develop the thermodynamic model of gas sorption in rubbery material with arbitrary strains. Multiple deformations are suggested for further study in order to generalize the model.

(2) The gas solubility is affected by temperature. In order to eliminate possible source of error, effective temperature control is strongly recommended in future work.

(3) The weight of sample used in this study is so small that the weigh gain of the sample cannot be measured accurately at low pressure. The weights are around 0.2 gram and 0.9 gram for silicone rubber and EPDM respectively; and the mass of sorbed CO_2 gas in silicone rubber and EPDM under $0.52MPa$ is about 2.0 mg and 5.5 mg. A bigger (heavier) sample will minimize the error of the weight measurement and is suggested for the future study.

(4) The initial delay when the sample was removed from the pressure vessel and placed on the analytical balance may affect the accuracy of the measurement. When taking out the rubber sample from the pressure vessel, the stress was removed suddenly. If such a change of stress state in rubber affects the rate at which gas diffuses out of the sample, this will result in an additional error. In order to minimize the error, this effect should be considered.

6. Bibliography

1. Zakaria. S. and Briscoe. B. J. Chemtech, August 1990, pp. 492-495.

2. Boot. J. C. and Naqvi. M. M. Plastic, Rubber and Composites Processing and Applications, Vol. 27. No. 9, 1998, pp.424-429.

3. Fleming, G. K. and Koros, W. J. "Dilation of polymers by sorption of carbon dioxide at elevated pressure. 1. Silicone rubber and unconditioned polycarbonate", Macromolecules, Vol. 19, 1986, pp. 2285-2291.

4. Lipscomb, G. G. "Unified thermodynamic analysis of sorption in rubbery and glassy materials", AICHE Journal, Vol. 36, No. 10, 1990, pp. 1505-1516.

5. Hill. T. L. Introduction to Statistical Thermodynamics, 1962, pp. 398-414.

6. Flory. P. J. Principles of Polymer Chemistry: Cornell University: Ithaca, NY, 1969, pp. 495-514 and pp. 577-580.

7. Pope, D. S., Sanchez, I. C., Koros, W. J. and Fleming, G. K. "Statistical thermodynamic interaction of sorption / dilation behavior of gases in silicone rubber", Macromolecules, Vol. 24, 1991, pp. 1779-1783.

8. Kamiya, Y., Natio, Y., Hirose. T. and Mizoguchi, M. "Sorption and partial molar volume of gases in poly (dimethyl siloxane)", Journal of polymer science: Part B: Polymer physics, Vol. 28, 1990, pp. 1297-1308.

9. Kamiya, Y., Natio, Y and Mizoguchi, K. "Sorption and partial molar volume of gases in polybutadiene", Journal of polymer science: Part B: Polymer physics, Vol. 27, 1989, pp. 2243-2250.

10. Kamiya, Y., Mizoguchi, K., Hirose, T. and Natio, Y. "Sorption and dilation in poly(ethylmethacrylate)-carbon dioxide system", Journal of polymer science: Part B: Polymer physics, Vol. 27, 1989, pp. 879-892.

11. Kamiya, Y., Terada, K., Mizoguchi, K. and Natio, Y. "Sorption and partial molar volumes of organic gases in rubbery polymers", Macromolecules, Vol. 25, 1992, pp. 4321-4324.

12. Kamiya, Y., Mizoguchi, K., Natio, Y. and Hirose, T. "Gas sorption in poly (vinyl benzoate)", Journal of polymer science: Part B: Polymer physics, Vol. 24, 1986, pp. 535-547.

13. Krykin, M. A., Bondar, V. I., Kukharsky, Y. M., Tarasov, A. V. "Gas sporption and diffusion processes in polymer matrices at high pressures", Journal of

polymer science, Part B: Polymer physics, Vol. 35, No. 9, Jul 15, 1997, pp. 1339-1348.

14. Kamiya, Y., Natio, Y., Mizoguchi, K., Terada, K. and Moreau, J. "Thermodynamic interactions in rubbery polymer/gas systems", Journal of polymer science, Part B: Polymer physics, Vol. 35, No. 7, May, 1997, pp. 1049-1053.

15. Briscoe, B. J., and Zakaria, S. "Interaction of CO_2 gas with silicone elastomer at high ambient pressures", Journal of polymer science: Part B: Polymer physics, Vol. 29, 1991, pp. 989-999.

16. Wissinger, R. G. and Paulaitis, M. E. "Swelling and sorption in polymer-CO_2 mixtures at elevated pressures", Journal of polymer science: Part B: Polymer physics, Vol. 25, 1987, pp. 2497-2510.

17. Xie, X. and Simha, R. "Theory of solubility of gases in polymers", Polymer international, Vol. 44, 1997, pp. 348-355.

18. Stannet, V. T., Koros, W. J., Paul, D. R., Lonsdale, H. K and Baker, R. W. Adv. Polymer Science. Vol. 32, 1979, pg. 71.

19. Wonders, A. G. and Paul, D. R. Journal of membrane science, Vol. 5, 1978, pg. 63.

20. Chan, A. H. and Paul, D. R. Polymer engineering and science. Vol. 20, 1980, pg. 87.

21. Koros, W. J. Ph.D. Dissertation, University of Texas at Austin, Austin, TX, 1977.

22. Crank, J. The Mathematics of Diffusion, Edition 1, 1956, pg. 45.

23. Treloar, L. R. G. The Physics of Rubber Elasticity, Edition 3, Clarendon Press, 1975. pg. 235.

24. Ogden, R, W. Proc. R. Soc. Lond. A. 326, 1972, pp. 565-584.

25. Reid, R. C., Prausnitz, J. M. and Sherwood, T. K. The Properties of Gases and Liquids, Edition 3, 1977, pg. 188.

26. Young, R. J. and Lovell, P. A. Introduction to the Polymers, Edition 2, 1991, pp. 141-145.

27. Mooney, M. Journal of applied physics. Vol. 11, 1940, pg. 582.

28. Rivlin. R. S. Phil. Trans. R. Soc. A241, 1948, pg. 379.

29. Arfken, G. Mathematical Methods for Physicists, Edition 3, Orlando, FL: Academic Press, 1985, pp. 964-965.

30. Koros, W. J. Journal of polymer science, Part B: Polymer physics, Vol. 23, 1997, pp. 1611-1985.

31. Horuiti, J. S. Journal of science. Pap. Inst. Phys. Chem. Res. (Jpn), Vol. 17, 1931, pg. 126.

32. Anthony, R. L., Caston, R. H. and Guth, E. J. Phys. Chem. Vol. 46, 1942, pg. 826.

33. Wall, F. T. J. Chem. Phys. Vol. 10, No. 132, 1942, pg, 485.

34. Hirose, T., Mizoguchi, K. and Kamiya, K. Polym. Prepr., Jpn, Vol. 34, 1985, pg. 8.

35. Kim, K-H., Cho, W-J., Ha, C-S., Kang, T-K. and Kim, Y. Journal of elastomers and Plastics, Vol. 29, No. 1, Jan, 1997, pp. 69-82

36. Ravikumar, H. B., Ranganathaiah. C. Kumaraswamy. G. N. and Thomas. S. Polymer, Vol. 46, No. 7, Mar 10, 2005, pp. 2372-2380.

Appendix A

Poisson's Ratio Measurement

Poisson's ratio is defined as the increment of the decrease in width divided by the increment of the length upon stretching for small deformation. Rubbers are usually thought to be incompressible materials, and the Poisson's ratio for an ideal rubber is 0.5. The measured Poisson's ratios at various stretch ratios for the rubbers used in this study are plotted in Figs. A-1 and Fig. A-2. Note that Poisson's ratio is the value at $\lambda \approx 1$, and values measured at higher stretch ratios deviate from this limit and are not representative of the Poisson's ratio.

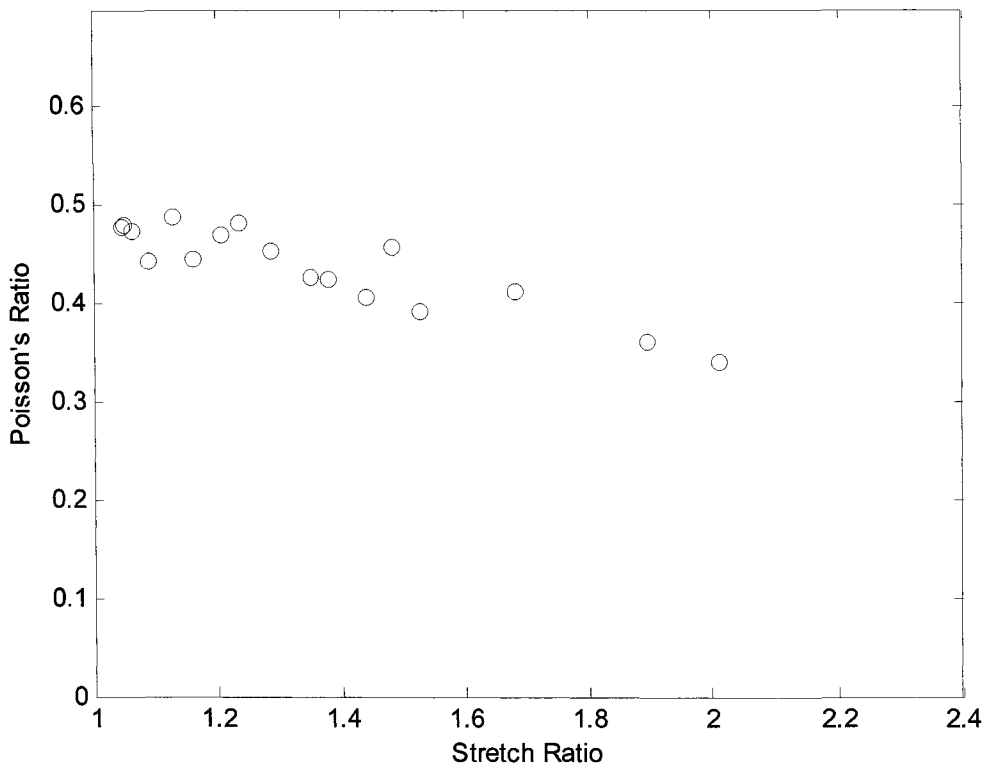

Fig. A-1 Poisson's ratio measurement of silicone rubber

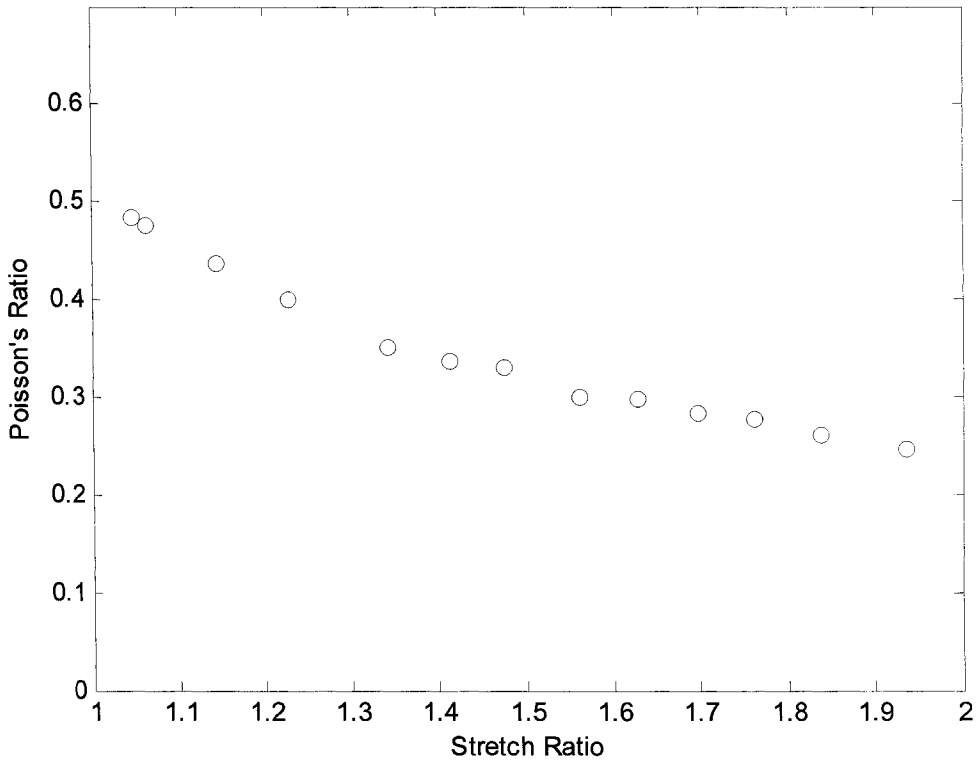

Fig. A-2 Poisson's ratio measurements of EPDM

Examining Figs. A-1 and A-2, it was found that the Poisson's ratio of silicone rubber and EPDM are close to 0.5 at small stretch, and slowly decrease as stretch increases. Thus it is reasonable to treat the silicone rubber and EPDM as incompressible materials.

Appendix B

DSC Measurement of Silicone Rubber

In order to measure the degree of crystallinity of silicone rubber, a DSC test was carried out with a heating rate 5°C/min. The results are presented in Fig. B-1 for silicone rubber.

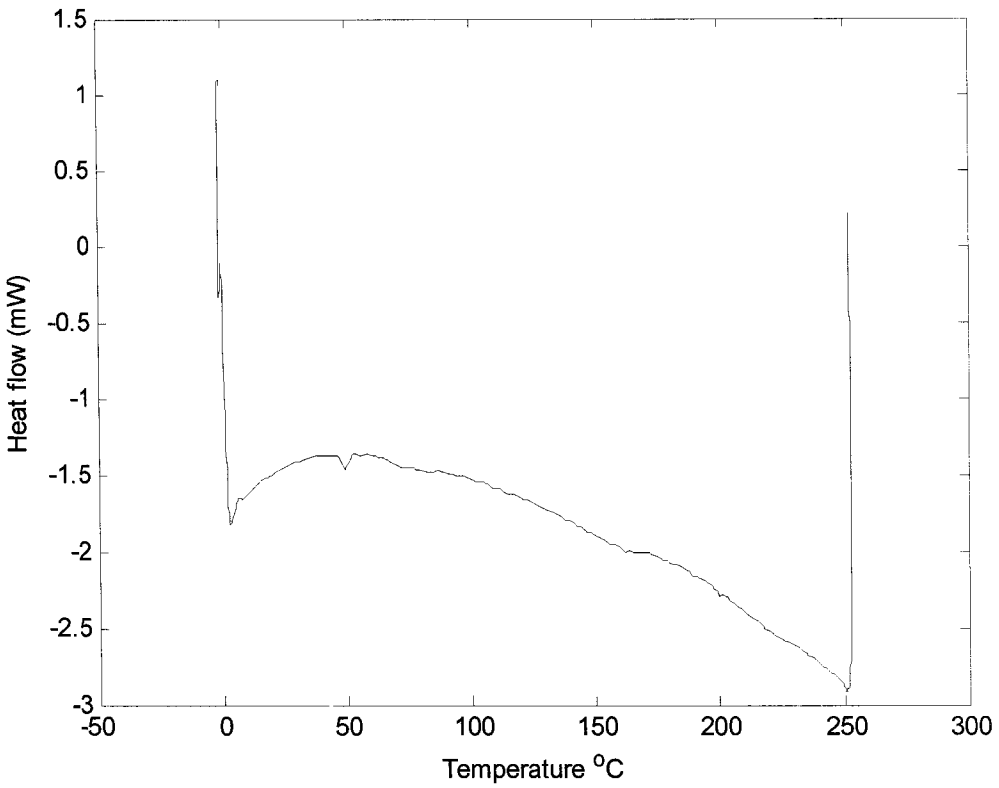

Fig. B-1 Silicone rubber DSC measurement data

Examining Fig. B-1, there is a small peak at about 50°C, which was thought to be the point that crystals formed. Usually, rubber is produced by reducing the temperature quickly. With rapid cooling, crystals do not have a chance to form. Thus, when the rubber is heated past the crystalline temperature, T_C, crystals are formed, which is shown in Fig. B-1. Thus, the degree of crystallinity of silicone rubber was determined to be zero.

Appendix C

Dimensions of the Frame

The dimensions of the frame used to hold the rubber band are given in Fig. C-1. In the middle of the main post, there are four strain gauges arranged in a full bridge (two strain gauges on each side). Only the main post and the two arms are shown in the figure.

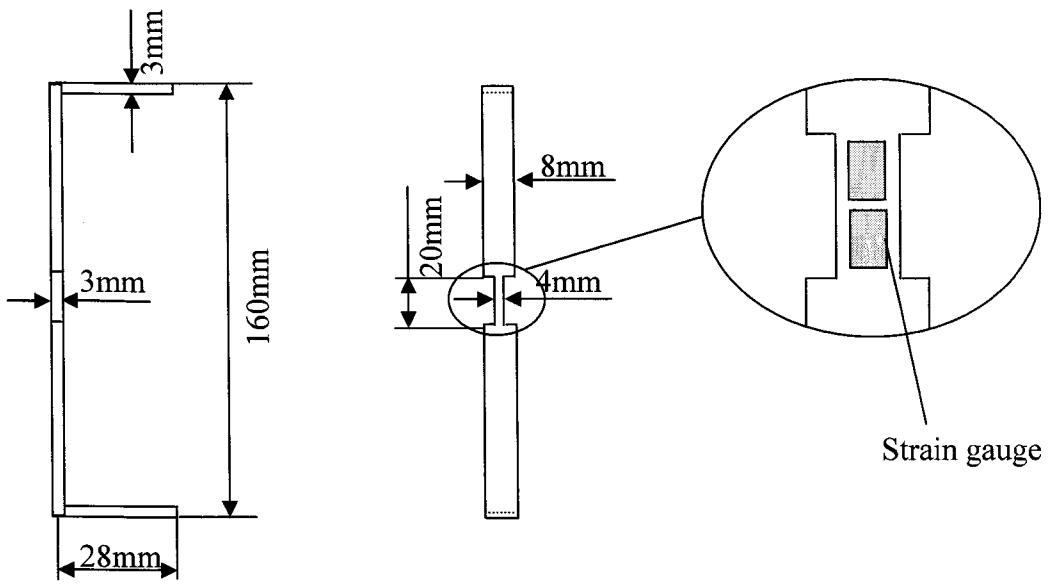

Fig. C-1 Dimensions of the frame that holds strain gages used in gas sorption measurement.